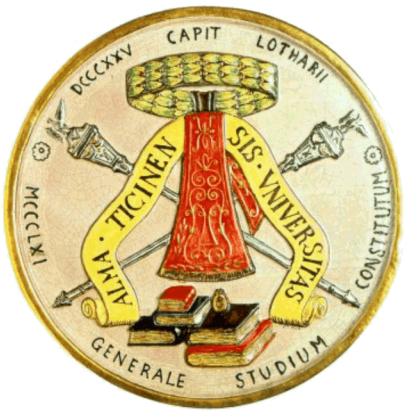

Università degli Studi di Pavia

Facoltà di Ingegneria

Corso di Laurea Specialistica in Ingegneria Biomedica

Finite Element Analysis of Coronary Artery Stenting

di

Federico Fogarotto

Relatori:
Prof. F. Auricchio - Università degli Studi di Pavia
Ing. M.Conti - Università degli Studi di Pavia

Anno Accademico: 2009-2010

Acknowledgments

First and foremost I offer my sincerest gratitude to Prof. Ferdinando Auricchio for supporting me throughout my thesis with his knowledge.
A special thanks to Ing. Michele Conti who was always willing to resolve my doubts and for the many hours devoted to my thesis.
I am very grateful to Istituto Mario Negri, especially to Dr. S. Previdi, and to D. Van Loo, from Ghent University, who provides me the images to work with.
I would like also to thank Dr. G. Sgueglia and Dr. A. Bartorelli for giving me the stent samples.
Finally, even if it would seem trivial, I've to thank my family and all my friends, for just being there.

Pavia, April 2011
Federico

Contents

Sommario

Fino a qualche anno fa, il concetto di "invasività" non rientrava nei termini più comunemente usati in Medicina. Con il progresso tecnologico e la messa a punto di innumerevoli tecniche diagnostiche e terapeutiche, le espressioni "indagine non-invasiva o poco o molto invasiva" sono divenute così usuali da essere utilizzate pressoché quotidianamente. Attraverso piccole incisioni, i chirurghi riescono a manovrare minuscole strumentazioni e/o a posizionare impianti nella regione interessata. La chirurgia mininvasiva ha portato principalmente ad una significativa riduzione delle cicatrici e ad una sempre minore degenza ospedaliera. Ogni nuova tecnica presenta vantaggi e svantaggi. La chirurgia mininvasiva richiede notevole praticità, ottenibile solo con l'esperienza, e possibili complicanze. Una stretta collaborazione tra chirurgia e ingegneria ha la possibilità di migliorare sotto molti aspetti gli impianti e le strumentazioni ad oggi utilizzate. L'applicazione di stent in arterie occluse è uno dei principali esempi di chirurgia mininvasiva analizzabili attraverso modellizzazioni computazionali. I modelli computazionali offrono un potentissimo strumento di ricerca per l'ottimizzazione delle principali proprietà degli stent, e consentono la comparazione di diverse tipologie. Simulazioni numeriche dell'espansione di stent in arterie stenotiche possono indirizzare chirurghi e ingegneri nella scelta dello stent che meglio si adatti al paziente.
In questa tesi è implementato un ambiente di progettazione virtuale per modellizzare stent coronarici. Partendo da immagini ad alta risoluzione, sono stati ricostruiti modelli tridimensionali realistici di stent, la cui espansione è ottenuta gonfiando un palloncino postovi all'interno. Tramite simulazioni numeriche di tali modelli si è analizzata la meccanica dell'espansione di stent coronarici. Si è sviluppata inoltre una strategia per l'impianto e l'espansione di stent in un tratto curvo di un'idealizzata arteria coronarica stenotica.

Chapter 1

Introduction

In this chapter the focus is on the treatments of coronary heart disease, in particular on the procedure of angioplasty and stenting. After a brief description of this disease, the typical treatments are described in order to understand why angioplasty is the main procedure applied nowadays. A short review of the evolution of the stenting techniques is then presented to provide a general view of the problems encountered in the development of such devices. Approaching stent implanting, the application field has necessary to be briefly described; therefore the coronary artery system is introduced. Finally the aim of the thesis is explained and its organization is summarized.

1.1 Atherosclerosis

Coronary heart disease (CHD) is now the leading cause of death worldwide. More than 7 millions people die each year from this disease. Despite improvements in survival rates, in the USA, 1 in 4 men and 1 in 3 women still die within a year of the first recognized heart attack[1].

Coronary heart disease is one of the most common and serious effects of aging. Fatty deposits build up in blood vessel walls and narrow the passageway for the movement of blood. The resulting condition, called atherosclerosis, potentially leads to blockage of the coronary arteries and a heart attack. Atherosclerosis is a focal inflammatory chronic disease that affects the elastic (e.g., aorta, carotid, iliac) and large to medium sized muscular arteries (e.g., coronary, popliteal). It involves a generic thickening and loss of elasticity of arterial walls thus hardening of the arteries. Small lesions are present in the coronaries of large part of population. But only in a small rate of these cases

such lesions evolve in a severe form till showing intense symptoms. It represents a real important problem, mainly related to the industrialized society's typical lifestyle.
Currently atherosclerosis is supposed to be an inflammatory response to the injury caused by an endothelial dysfunction [2]. Atherosclerosis consists in the formation of plaque in the arterial walls, called atheroma, fibro-fatty plaque or atherosclerotic plaque, i.e., an thickening of intima (the closest layer to the lumen in vessel walls). Its pathogenesis is complex but it can be described in a simple way, since these plaques undergo a general slow evolution: first are composed of lipids, mainly cholesterol, then plaques become larger and larger building a support structure composed of fiber and connectival cells, resulting in an occlusion of the artery, the so-called stenosis [2].
Lipids' accumulation on arterial walls, that slowly increase in volume, reduce wall's elasticity and occlude blood flow. As the impediment to blood flow grows, the blood supply to the downstream tissues and organs becomes insufficient and the lack of oxygen can cause severe complications involving arts, brain and heart.

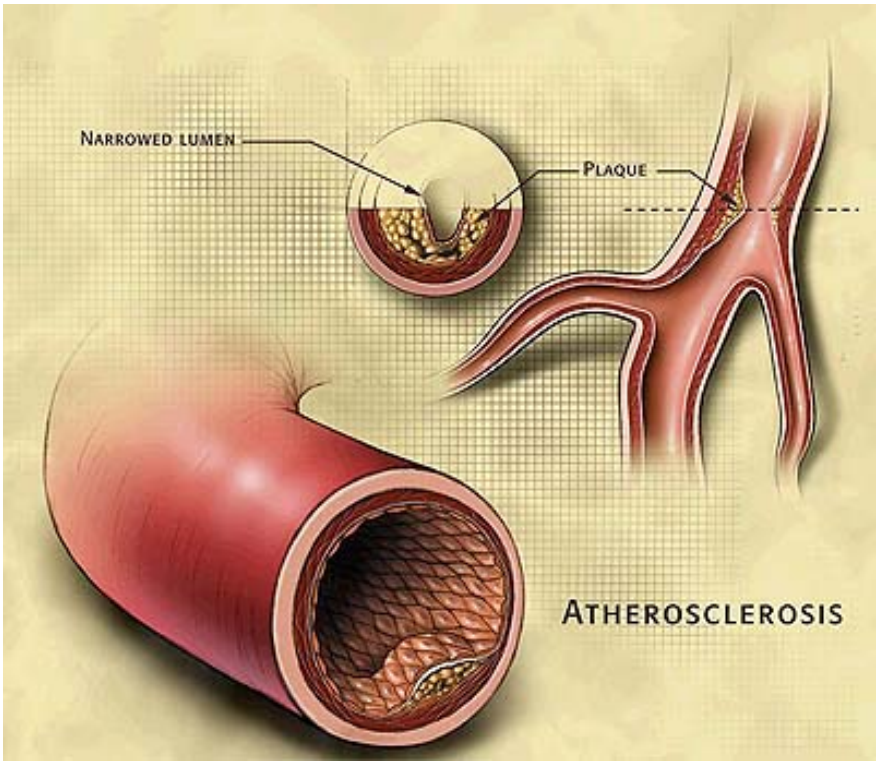

Figure 1.1: A) A normal artery with normal blood flow. B) An artery with plaque buildup.

Atherosclerosis can affect almost any artery in the body. But in the heart its effects can be crucial. The body depends on a strong pumping heart to circulate life-giving

blood, and this includes to the heart muscle itself. If the coronary arteries become blocked, the cardiac muscle begins to fail, and so the blood circulation decreases, reducing also the circulation to the heart muscle itself.
Loss of elasticity, that leads to an increasing of blood systolic pressure, and the occlusion of the artery, are not the only consequences due to the build-up of the plaque. An inflammation process occurs and the following rupture of this collection of fatty materials leads to more severe pathologies. Indeed atherosclerosis is the cause of severe pathologies such as heart attack and stroke. The cardiovascular risk is thus related both to plaque's size and to its inflammation. Relatively small plaques with a high inflammation level are more dangerous than larger plaque with no inflammation.
When a part of the plaque breaks, the blood and cholesterol come in touch. This process leads to the formation of a clot, as it happens when we hurt ourselves. Inside the artery, coagulation mechanisms give then rise to a hard substance (thrombus or clot) that can block blood flow resulting in a sudden enlargement of the plaque. Due to this lesion a small piece of the ateroma can break off and move through the affected artery to smaller blood vessels, blocking them and causing tissue damage or death (embolism).
Different treatment options are available for coronary atherosclerosis; the main procedures are: the bypass surgery, the angioplasty and the stent placement. In the following section a brief description of each of these options will be addressed.

1.2 Treatment options for coronary atherosclerosis

Lifestyle changes are often the best treatment for atherosclerosis. But sometimes, medication or surgical procedures may be recommended as well. Various drugs can slow down - or sometimes even reverse - the effects of atherosclerosis although too often more aggressive treatment is needed. Severe coronary heart disease needs bypass surgery or angioplasty.

Coronary Artery Bypass Grafting (CABG), generally called bypass surgery, is the surgical creation of a new blood flow path by re-routing the flow of blood thus overcoming the blockage, as can be visualized in Figure 1.2. The bypass graft enables blood to reach the heart by flowing around the blocked portion of the diseased artery. In order to avoid rejection, segments of saphenous vein or internal mammary artery are used to build this bridge. This procedure is very invasive as it is often needed, not

just a sternotomy, but also to stop the patient's heart and connect it to the heart-lung machine for extra corporeal circulation.

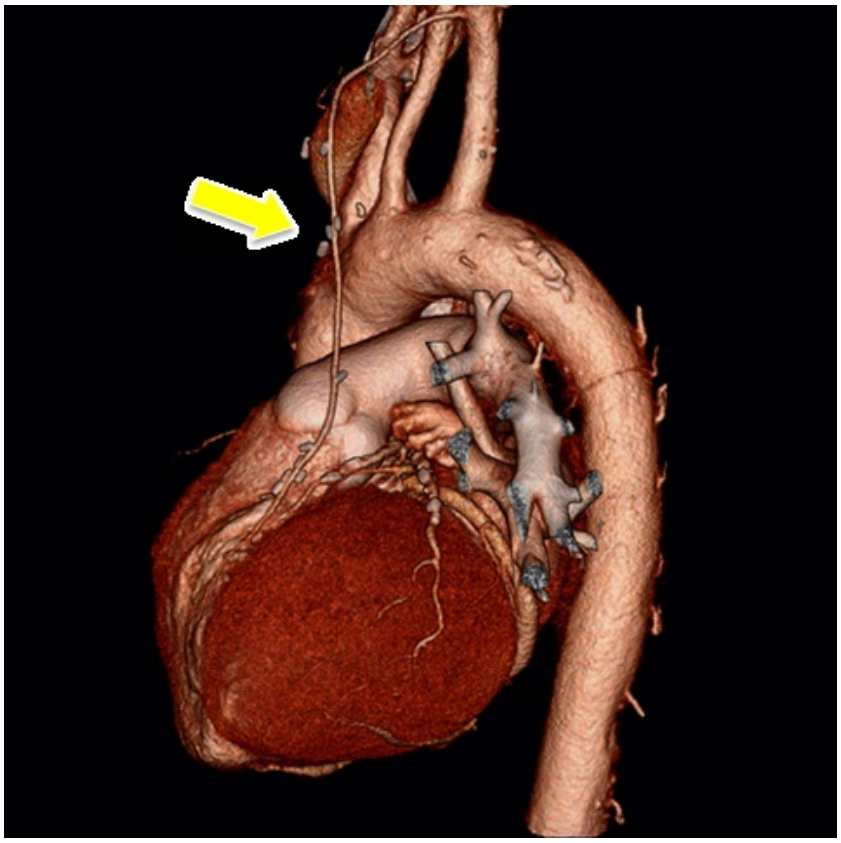

Figure 1.2: Bypass surgery. The bypass graft enables blood to reach the heart by flowing around (bypassing) the blocked portion of the diseased artery. Saphenous vein or mammary artery are used to build this new blood flow path.

Percutaneous Transluminal Angioplasty (PTA) [1] is a minimally invasive procedure aiming at reopening a blocked o narrowed vessel. Using imaging techniques, a balloon-tipped catheter (i.e., a long thin plastic tube) is guided into an artery or vein and advanced to target lesion. The balloon is inflated compressing the plaque against the artery walls enlarging the vessel's occlusion, then it is deflated and removed, as shown in Figure 1.3. In order to prevent the vessel's re closure, a metallic scaffold, called stent, is placed in situ to support arterial walls. Inflating the balloon deploys the stent, which remains expanded to keep the vessel opened.

[1] also known as PCI Percutaneous Coronary Intervention and PTCA Percutaneous Transluminal Coronary Angioplasty

Instead of pushing the plaques against the arterial wall as in angioplasty, there are other procedures, generally joined under the name Atherectomy, that physically remove the plaque (e.g., in the rotational atherectomy, a rotary device,-a high-speed cutting drill mounted on a catheter- called rotoablator, that literally shaves off plaque from an artery wall). The main reason for using an atherectomy device is to traverse small and tortuous coronary arteries that are difficult to navigate with thin angioplasty guide wires alone. Indeed sometimes angioplasty is preceded by atherectomy.

1.3 Angioplasty

Patients with severe CHD have traditionally been treated first with drug therapy and then, if necessary, with coronary artery bypass surgery. The introduction of angioplasty and stenting have opened new views for successful treatment of CHD with techniques being far less invasive than traditional surgery. Rather than constructing a new route for blood flow, as in bypass surgery, these procedures open or widen existing ones. From its introduction (Dr.Gruentzig, 1977), PTCA has been adopted worldwide, growing from few procedures to 1.5 million only in Europe [3].

As depicted in Figure 1.3, the procedure is simple:

- Through a small incision in the femoral artery[2], a Teflon-coated catheter is inserted and threaded to the vessel obstruction;
- A thin, flexible guide wire is moved in the guiding catheter beyond the afflicted area;
- A balloon catheter is moved over the guide wire and accurately positioned in the blockage;
- The balloon mounted on the distal tip of the catheter is inflated;
- The plaque is compressed by the balloon and the arterial lumen is restored;
- The balloon is deflated and then removed with the catheter, leaving the vessel widened.

[2]90% of PTCA are done from the femoral approach but can be done also from brachial or radial artery

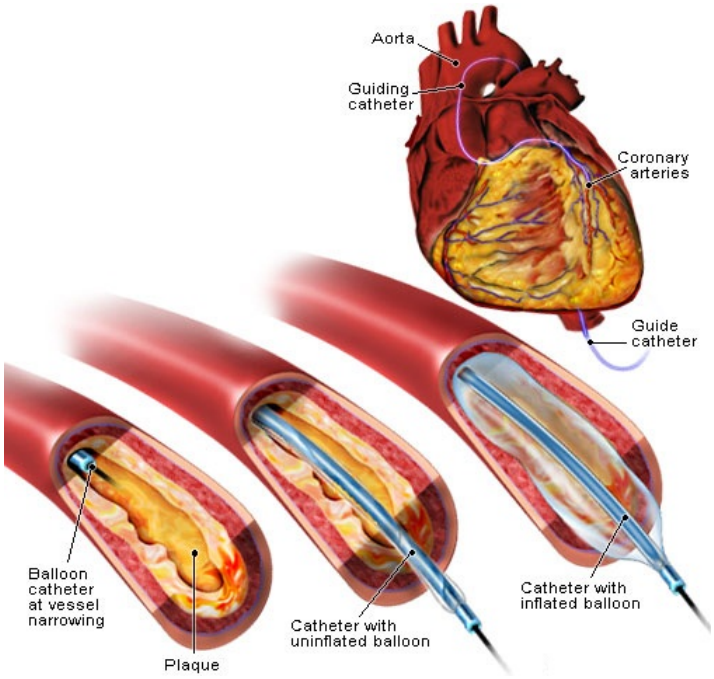

Figure 1.3: Basic step representation of an angioplasty procedure. Using imaging techniques, a balloon-tipped catheter, a long, thin plastic tube, is guided into an artery or vein and advance it to where the vessel shows a stenosis. The balloon is inflated, compresses plaques against the artery walls enlarging the vessel's occlusion, then deflated and removed.

Complete recovery of the vessel lumen would be the ideal result of an angioplasty, but the more typical result is a 30% residual lumen stenosis [4].
In order to avoid the elastic recoil of vessel walls, as the balloon is removed, the tissue damage (arterial dissection and abrupt closure) and the possible restenosis, a stent is placed on the balloon. The stent acts as a support to the arterial wall: as the balloon is gradually inflated, the stent expands, embeds itself into the arterial wall and, after the balloon deflation, is left in situ to prevents the plaque to reclose (see Figure 1.4). The stent's wire mesh, in its expanded state, allows to maintain a pathway for blood flowing minimizing the contact between the arterial walls.
Stents are crimped on a folded balloon (generally three-or-six-folded balloon) to reduce the crossing profile in order to reach each stenotic region.

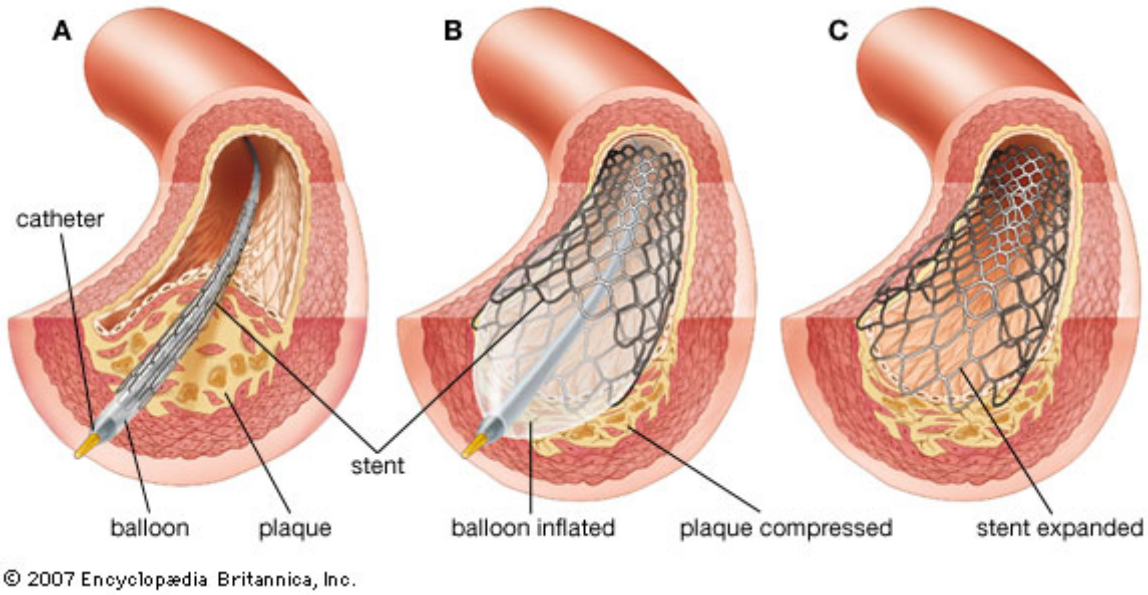

Figure 1.4: Stent insertion and deployment. A: The delivery system is placed in stenotic region. B: As the balloon is gradually inflated, the stent expands, embeds itself into the arterial wall. C: After the balloon deflation, the stent is left in situ to prevents the plaque to reclose.

1.4 Angioplasty/Stenting vs. Bypass

Many studies have shown that stenting presents higher rate of revascularization than bypass surgery, but the rates of death and myocardial infarction were similar in the first years post-procedure [5, 6]. The Stent or Surgery (SoS) trial [7], reporting on six years of follow-up data, shows a persistent survival benefit in CABG patients.
The advantage of the angioplasty procedure is that it is a faster and less invasive method to treat atherosclerotic plaque buildup. Angioplasty patients experience a quicker and less painful recovery. The procedure requires only a few days in hospital and recuperation time is minimal. Coronary artery bypass surgery, which involves opening the chest cavity, requires instead several hours under general anesthesia and necessitates a week or two in the hospital, followed by several weeks more of recuperation for a patient to heal completely at home.
Although balloon angioplasty sounds like the first choice to treat CHDs, it is not right for everyone. The presence of coronary heart disease does not automatically qualify a candidate for angioplasty. Indeed, not all plaques are suitable to the angioplasty

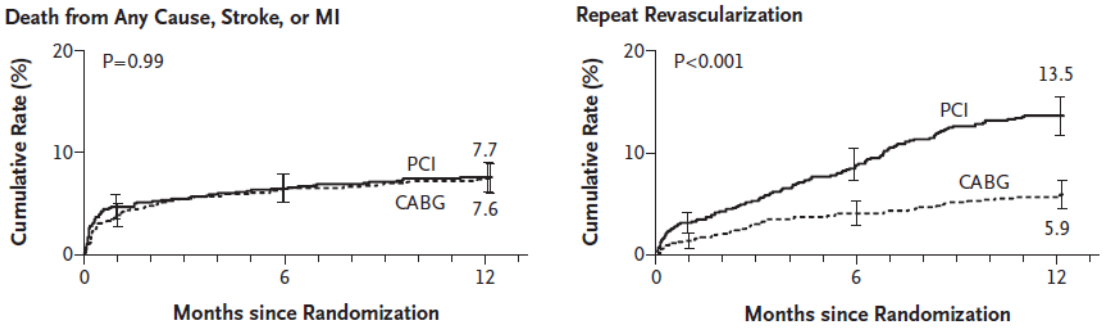

Figure 1.5: Rates of outcomes among the Study patients, according to treatment group (PCI and CABG). The two groups had similar rates of death from any cause, stroke, or myocardial infarction (MI)(relative risk with PCI vs. CABG, 1.00). In contrast, the rate of repeat revascularization was significantly increased with PCI (relative risk, 2.29)[6].

technique. Lesions vary in size, location, and composition; some of them are too long or too much calcified for angioplasty. Some lesions are difficult to reach with a balloon-tipped catheter. In other cases, the guide wire, used to thread the balloon catheter into the vessel, may be unable to penetrate the hardened plaque which occludes completely the artery. A patient with stenosis in three or more coronary arteries is generally a better candidate for bypass surgery.

1.5 Coronary stenting: the evolution of stenting

Most lesions that can be stented are stented [4].
Despite the immediate positive results and the progressive improvements in angioplasty, in almost 30-40% of patients, the artery has to be widened again at 6 months [8]. Restenosis is due to the elastic recoil of arterial wall and mainly to the so-called negative remodeling: the healing response to balloon inflation if excessive, may narrow again the vessel losing the achieved lumen diameter. Moreover the balloon's expansion causes an immediate injury to the arterial wall, called dissection. Although dissection is an intentional injury, since the balloon's inflation has the goal to remove the atherosclerotic plaque and enlarge the vessel, this may lead to the total occlusion of the vessel, the abrupt closure (incidence of 5-6% [4] and [9]). As said, to avoid these complications has been introduced an endovascular prosthesis called stent. Stents are metallic scaffolding meshes that are deployed within a occluded coronary artery to keep

it open, providing a mechanical support and contrasting the aforesaid phenomena.
From Charles Dotter's idea to FDA approval (Palmaz-Schatz balloon-expandable stent in 1994) have passed many years, but now we are in the stent era. Indeed stent placement is now performed in 80% of percutaneous revascularizations [4].
Efficacy comparison of stent implantation with angioplasty, in two landmark clinical trial the STRESS and the BENESTENT studies [10, 11], shows a lower restenosis rate in the "stented" group (31.6% vs. 42.1% and 22% vs. 32%). Stents differ in their composition (e.g. stainless steel, cobalt-chromium, nitinol), design (e.g rings, coils), mode of implantation (balloon-expandable, self-expanding) and treatment (coated stents, drug-eluting stents, bioabsorbable stents) but each stent must combine high flexibility and low crossing profile, the path to stenosis is almost always tortuous and tight, with good radial strength, to bear the elastic reaction of the vessel, and with biocompatibility (see Table 1.1).

Feature of an ideal stent
Corrosion resistance
Low thrombogenicity (biocompatible)
Radiopacity
Easily positioning
Flexibility
High Radial strength
Low elastic recoil
Uniformity (to avoid dogboning and foreshortening)
Minimal surface area (less contact metal-vessel wall)
Low crossing profile
Low Cost

Table 1.1: Feature of an ideal stent.

With respect to deployment mechanics, stents can be classified as: i) balloon-expandable; ii) self-expanding. Balloon expandable stents are mounted on a balloon which is gradually inflated driving the stent deployment. Self-expanding stents are manufactured at the vessel diameter, then crimped and constrained in the delivery system; during the deployment the self-expanding stent is gradually released from the catheter recovering the target diameter thanks to its mechanical properties. This expansion process is due to a nickel-titanium alloy (nitinol), whose main feature is the shape memory. Self-expanding stents are very flexible and have a significant radial

force. They are typically used when the artery is particularly long, tortuous or disconnected (such as the external iliac artery and the femoral artery) and in the presence of plaques easier to open.

As reviewed by O'Brien and Carroll [12], in the early stent development, the main goal was the thinning of struts to make the stent able to reach the target vessel. Reducing the struts thickness without losing radial strength has led to the introduction of new materials: cobalt-chromium alloy (*Multi-Link Vision* coronary stent from Abbott Laboratories), the *Driver* coronary stent's MP35N alloy (cobalt-chromium-nickel-molybdenum, from MedTronic Inc.), tantalum (sandwiched between two layers of stainless steel in the *TriMaxx* stent from Abbott Laboratories) and stainless steel with platinum additions (*Element* from Boston Scientific Corp.).
From the strut thinning, the focus has been then moved to the biocompatibility. The major complication encountered with the stenting procedure was, indeed, the potential thrombogenicity, due to the interaction between blood, tissue and stent surface and the in-stent restenosis (ISR). Stent deployment, due to the high pressure, causes a lesion in the arterial wall damaging not only the tunica intima but also the tunica media, generating an additional a stimulus to platelet aggregation, already activated by the thrombogenicity of stent's metallic surface. Subacute stent thrombosis was easily reduced with antiplatelet therapy with aspirin and ticlopidine [13].

Despite stenting technique reduces the rates of restenosis compared with PTCA, ISR still occurs in 25% of patients. ISR is a result of three main processes [13]:

- Immediate vessel recoil after stretch injury;
- Negative arterial remodeling;
- Neointimal hyperplasia [3];

In-stent restenosis, beside restenosis due to angioplasty, is related also to chronic action of the stent wires. The incidence of ISR is even higher in cases where stents are implanted in small vessels, long and bifurcation lesions or in patients with diabetes mellitus [14]. To overcome this problem many techniques have been tested such as brachytherapy (a radiation therapy to stop the cellular proliferation), atherectomies and laser ablation but no one was really able to reduce ISR [15]. A variety of inorganic coatings has been explored in order to reduce restenosis, from carbon coatings

[3] vascular injury due to the stent deployment activates smooth muscle cells from the tunica media, so they proliferate and migrate into the intima producing collagen and extracellular matrix that narrow the lumen again.

to titanium-nitride-oxide coating passing through silicon carbide surface minimizing metal ion release but restenosis still persisted [12]. The only way to manage ISR was the use of antiproliferative drugs in the occluding region, this open the way to the introduction of drug-eluting stents (DES). A drug-eluting stent, as its name says, is a stent that locally deliver an appropriate agent able to prevent restenosis. It consists of three components: (i) a metallic platform, (ii) a drug carrier able to store a therapeutic compound through the path to the target lesion and to release its contents at the right time and in controlled doses, (iii) an effective drug that inhibits the neointimal growth. Most of these systems use synthetic polymers as reservoir for the drug such as silicon, cellulose esters, polyurethanes, PVA, PMMA and PLLA. The first generation of DES was represented by heparin-coated stents, since its anticoagulant effect can prevent thrombus' formation. Numerous pharmacologic agents have been incorporated on the stent surface, as stated by Htay and Liu [13]. The compounds have either anti-inflammatory, antiproliferative or antimigratory properties. The most promising has proved to be sirolimus, since it manages to arrest the smooth muscle cells' proliferation and migration preventing the neointimal hyperplasia, and the taxol, able to enhance microtubule stability and therefore stopping cell division and proliferation. Currently only few systems are available on the market: the sirolimus-eluting *Cypher* stent from Cordis Corp.(a Johnson and Johnson Company), the paclitaxel-eluting *Taxus* stent and *Liberté* from Boston Scientific, the *Xience V* Everolimus-eluting stent and the *Endeavor* zotarolimus-eluting stent from Medtronic. With the introduction of DES, the ISR has been considerably reduced from over 30% to the range 4-15% [14]. As cited by Htay and Liu [13], DES cost approximately three times the BMS (1000$ vs. 3000$), but in cost-effective analysis the difference between the groups at 1 year was little.

Even if restenosis has been limited, it is known that permanent stent cause limitations including long-term endothelial dysfunction, delayed re-endothelialization, thrombogenicity, permanent physical irritation, chronic inflammatory local reactions, mismatches in mechanical behavior (vasomotion) between stented and non-stented vessel areas, inability to adapt to growth, and importantly nonpermissive or disadvantageous characteristics for later surgical revascularization [14]. That's why the next step in stent development is the bioabsorbable stent: a stent made by biodegradable material to avoid all the potential long-term complications above described. Although polymers used are not able to guarantee the same radial strength compared with bare metal stents (BMS) and it is not known how long the stent has to remain in situ before starting degrade, the first trials using bioabsorbable magnesium alloy stent have proved to

be safe and promising [14]. It has been chosen a magnesium alloy since magnesium has a variety of advantages: acts as a vasodilator, it's involeved in muscle contraction and its slow degradation releases little harmless concentration.

Despite the introduction of all these innovations in stenting techniques, the vascular injury is not eliminated. This damage, caused by stent insertion, is due to both stent-artery and balloon artery interactions, both depending basically on stent design. Vascular injury is higher at the stent ends since the balloon and the stent expand in a non-uniform ends-first manner (the dogboning effect), shorten while deploying (the foreshortening effect) and the balloon comes in touch with the artery, being longer than the stent [16].

From the concept of a scaffolding structure placed in coronary artery in order to avoid its reclosure, stenting has emerged as the dominant technology for catheter-based coronary revascularization. Coronary stenting had an exponential growth in the last three decades, in terms of number of procedures, design and materials used. The technological improvement associated with a better understanding of the pathophysiologic mechanisms of coronary arteries' disease, has allowed the development of a wide variety of stents, all characterized by increasing security, ease of use and clinical effectiveness.

1.6 District of stenting

The blood vessels in which plaques cause the worst effect are the coronary arteries, whose size is fairly (quite) small (ranging from 3 to 6 mm). It results in a greater possibility of occlusion compared to other arteries with risk of angina pectoris and myocardial infarction. Therefore in most cases, the surgical intervention affects the coronary arteries. Nowadays, stents are mostly placed in the treatment of arterial revascularization, but are also used to widen other tubular structures anywhere in the body: veins, bile duct, carpal tunnel, esophagus, colon, trachea, bronchi, ureter and urethra.
The coronary arteries supply the heart with oxygen and nutrients (blood). The name of these small vessels comes from their particular distribution around the heart, coronaries act as a crown that surround cardiac muscle. The coronary anatomy has a great variability: coronary arteries vary in length, size and branches in each person but generally are two: the left main coronary artery (LCA) and the right coronary artery (RCA). Both originates from ascending aorta, the LCA from the left coronary sinus

of Valsava and the RCA from the right coronary sinus. The coronary tree contains many bifurcations. While the right coronary artery remains undivided (except the branches departing from it) throughout its path around the heart, the left coronary artery splits in the left anterior descending coronary artery (LAD) and left circumflex coronary artery (LCX). Both LAD and RCA are divided into proximal, mid, and distal segments.

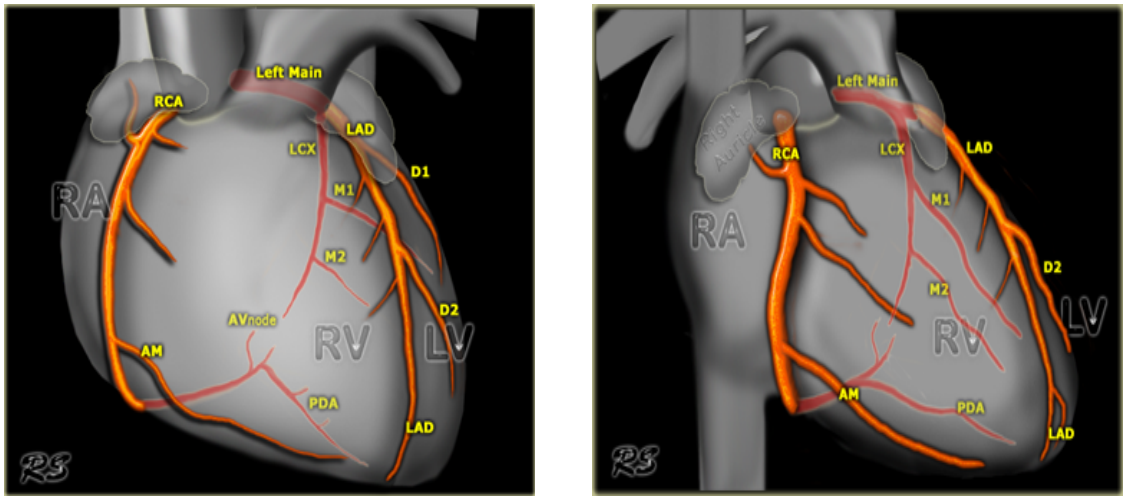

(a) RCA, LAD and Cx in the anterior projection

(b) RCA, LAD and Cx in the right anterior oblique projection

Figure 1.6: Schematic representation of the main coronary arteries. RCA: Right coronary artery; LAD: Left Main or left coronary artery; LAD: Left anterior descending; D1,D2: Diagonal branches; LCX: Left circumflex; M1,M2: Marginal branches; AM: Acute marginal branch; PDA: Posterior descending artery.

Due to the pulsatile flow, the dimensions and geometry of coronary arteries and the cardiac muscle activity, the hemodynamic conditions at the point where branches split are very complex. This leads the coronary bifurcation to be extremely susceptible to atherosclerosis. Coronary bifurcation lesions are involved in up to 15-20% of all PCI procedures [17].

1.7 Aim and organization of the thesis

Given this short review about stenting, the main aim of this thesis is to investigate the behavior of a variety of balloon-expandable stent designs through modeling stent insertion and deployment using the finite element method. In particular the focus is on bare metal stents in coronary lesions. This work is organized as follows:

- **Chapter 2: Stent Modeling**

  Understanding the existing knowledge about stent delivery system is crucial to start 3D-modeling. Therefore the basic principles of the stent system are briefly described, especially regarding the main features of the balloon and the stent. The Finite Element Analysis is then presented since it is perfectly suitable to study the biomechanical behavior of the stent, followed by a short review on stent deployment modeling. Finally the procedure to generate a three-dimensional finite element model of balloon expandable stent, starting from micro-computer tomography scans, is addressed. The development of accurate computer models to study stents is essential to efficiently investigate many different stents and implantation techniques. Creating a stent model based on an available stent begins with an accurate determination of the stent and strut dimensions and the generation of the CAD (Computer Aided Design) model corresponding with the stent.

- **Chapter 3: Balloon expandable stent deployment**

  A first step to study the stenting procedures using finite element analysis is to develop validated models to study balloon-expandable stents. Therefore, a realistic model to investigate the free stent expansion is developed. First a realistic and validated model is developed to study the expansion of the folded angioplasty balloon, subsequently a whole stent system model is developed. This model serves as a solid basis to study and optimize the mechanical behavior of balloon-expandable stents as the numerical results correspond very well with both qualitative and quantitative manufacturer data. The efficiency and accuracy of the developed procedure is illustrated for the Cordis's Cypher stent.

- **Chapter 4: Stent insertion and deployment in a coronary artery**

  Since the stent has to deploy into an occluded artery, simulations of the stent insertion and interaction between stents and coronary vessels have to be developed. In this chapter, a simulation strategy considering the insertion of a folded balloon catheter over a guide wire is proposed in order to position the stent within the straight and curved vessel and then let it expand. Furthermore the deployment models of the Element and the Tryton stent are addressed.

- **Chapter 5: Conclusion**

  The final chapter gives an overview of the major findings of the describeb research activity and contains some guidelines regarding stent design and selection. In addition, some suggestions for further research are included.

Chapter 2

Stent Modeling

The aim of this chapter is to develop a 3D realistic model to study the deployment of balloon-expandable stents. Before creating a model of the stent expansion, is necessary to highlight the main features of each component that builds up the entire device. Therefore an explication of the key characteristics of the balloon and the stent is addressed. Then a short review on modeling stent deployment is presented, followed by a brief explanation of the finite element analysis till reaching the description of how the 3D model is built.

2.1 The delivery system

As stated in Chapter 1, the delivery system has to be guided through the small and tortuous arterial tunnels in order to reach the target lesion. Consequently its main features have then to be the flexibility and the trackability[1]. The delivery system is composed by a guide wire, a tipped balloon and a crimped stent. The guide wire is moved beyond the stenosis and acts as the rail for the advancement of dilatation equipment i.e., balloon and stent. Guide wires are made by a nitinol core around which is wrapped a Teflon-coated stainless steel wire as a spring coil [4] to decrease the contact area between the surface of the guide wire and the tissue. Guide wires are available in different lengths and diameters, but standard size ranges from 0.09 to 0.1 cm (0.035-0.038 inch) with respect to diameter and from 145 to 160 cm with respect to length [18].

[1] the ability to advance through the turns of arterial segments

2.1.1 Balloon

Modeling stent deployment passes through the creation of a balloon model. The balloon must have thin walls, so it can be tightly wrapped around a catheter shaft minimizing its profile, and high strength, to undergo high pressure without breaking off, with relatively low elongation. A standard balloon, as depicted in Figure 2.1, consists of a cylindrical body and two conical tapered ends, whose diameter decreases from the diameter of the balloon to the one of the catheter shaft, a tiny tube passing inside the balloon. PTCA balloons are high pressure balloons since they are used to apply force whether to compress the plaque or to deploy the stent.
The balloon is capped with two short tubular tips, one cylindrical and one conical, placed to track the balloon along the guide wire.

Figure 2.1: Balloon inflated: a standard balloon consists of a cylindrical body and two conical tapered ends.

To characterize an angioplasty balloon three main features have to be taken into account:

- Dimensions;
- Material properties;
- Design (folding pattern).

Balloon dimensions

Balloon are produced in a wide range of diameters, lengths and shapes suited for use in a broad range of minimally invasive procedures. Typical PTCA balloon are available from a variety of manufacturers with diameters of 2.0 to 4.0 mm and 10 to 40 mm long, to match the size of the coronary lesion. When referring to balloon dimensions and features, it is necessary to clarify the meaning of some keywords. As speaking of balloon diameter, it's referred to its expanded configuration not to the wrapped configuration, which is named, instead, balloon profile. Table 2.1 explains the meaning of some significative terms.

Balloon Diameter	Nominal inflated balloon diameter measured at a specified pressure
Balloon Length	The working length (i.e., the length of the straight body section)
Rated Burst Pressure	Maximum statistically guaranteed pressure to which a balloon can be inflated without failing
Balloon Profile	Maximum diameter of the balloon when mounted on a catheter in its deflated and wrapped condition
Balloon Compliance	Change in balloon diameter as a function of inflation pressure

Table 2.1: Balloon Keywords: as approaching balloon modeling some terms has to be explained to make clear their specific use[19].

Balloon is always longer than the stent and, as shown by De Beule [16], this overlength influences the expansion; a balloon long as the stent does not expand showing dogboning, while a balloon longer than the stent opens in a first-end manner. Since the dogboning and the balloon overlength are causes of vascular injury (as explained in section 1.5), the balloon length should be kept as small as possible.

Balloon folding pattern

A standard balloon consists of a cylindrical folded body and two conical tapers ending in circular bases giving the balloon a sausage shape. The stent deployment is also conditioned by the folding pattern. Indeed to deliver to the stent system through vessels, the balloon is folded around the catheter that passes through it, thus minimizing the

crossing profile. Folds can vary from 3 to 6, the more folds the balloon has, the lower profile is reachable and more uniformly the stent opens [16].

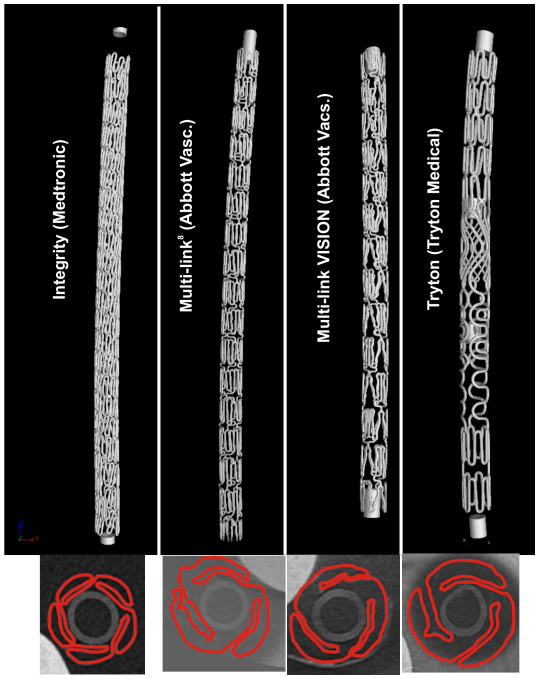

Figure 2.2: Balloon Design. Top: Different balloon folding pattern obtained from micro-CT images. Bottom: Stent cross-section. With micro-CT images is possible to reconstruct a 3D model of a stent.

Balloon materials

The most important feature of the balloon is its ability to inflate to a precisely defined diameter under high pressures in order to ensure that the balloon will not continue to expand and damage the arterial walls. This property is due to the material and it's called compliance. Balloons are molded to their inflated geometry from noncompliant or low-compliant materials but, since compliant balloons oversize and rupture at pressures as low as 1 MPa, semicompliant and noncompliant balloons have been chosen for angioplasty procedure. Semicompliant balloons, such as that manufactured from polyethylene or nylon, grow by less than 10% once reached their nominal diameter (at 1 MPa circa) (e.g., a 3.0-mm balloon growing to 3.2 mm), whereas noncompliant balloons such as that manufactured from polyethylene teraphalate (PET) can retain their defined diameter up to 2 MPa to allow the expansion of coronary stents[4, 19].

The compliance chart, given from all the manufacturers, provides the range of inflation and must be followed to prevent balloon rupture. This pressure typically from 2 to 20 atmospheres, is specified in terms of the *Rated Burst Pressure*. Taking any balloon catheter above its rated burst pressure increases the risk of balloon rupture, with the potential for air embolization, local dissection, or difficulty in removing the balloon from an incompletely dilated lesion [4].

The choice of the balloon material depends on the size: the larger the diameter, the lower the rated pressure. This is due to the fact that as the diameter of the balloon increases, the stress in the balloon wall increases when inflated to its nominal diameter. PET is ultra-thin-walled, ranging from 5 to 50 microns (0.0002" to 0.002"), it is capable of producing balloons of extremely low profile with high strength. Besides nylon high-pressure balloons are softer than PET balloons, although not as strong, thus requiring a thicker wall for a given burst pressure. This generally means that nylon balloons will have a larger profile than PET upon insertion into the body but because the material is softer, it is more easily refolded[19].

2.1.2 Stent

As described in Table 1.1, stents must provide some factors, such as flexibility, high radial strength, low crossing profile, biocompatibility and radiopacity, that play a crucial role in the clinical and design choices of a stent. Delivering stents into the body from vascular access requires the stent to be very flexible and to have the lower crossing profile. Deploying the stent in the stenosed vessel requires, instead, the stent to have high radial strength, to keep the vessel opened, low elastic recoil, and provide optimal scaffolding to avoid arterial walls to prolapse within the stent struts.

Stent materials

Stents are manufactured with materials that can be plastically deformed when the balloon is inflated, so the stents can stay in its deployed configuration once the balloon is removed. Such materials must also provide minimal elastic recoil and high radial strength to withstand the stresses imposed by the elastic recoil of the arterial walls. To achieve these features the material should have low yield stress to allow the balloon-stent deployment, and high elastic modulus (Young's modulus), to ensure minimal elastic recoil. Balloon expandable stents are manufactured in the deliverable configuration, crimped on the balloon, ready to be expanded as they reach the target site inside the vessel. Self-expanding stents, on the other hand, are manufactured in the

expanded shape, then compressed and constrained in a delivery system. It's therefore clear that materials used to build stents differ from typologies of stents; balloon expandable stents are most widely made by stainless steel, while in self-expanding stents the shape memory alloy Nitinol has the leadership. The continuous technological improvement in stenting has brought out different superalloys such as Cobalt Chromium, Tantalum and other proprietary materials such as the PtCr of Boston Scientific Corp to challenge the classic stainless steel. Despite the thinner struts and low profile achieved with this new materials, the stainless steel, in particular the variety 316L, is the most common material chosen to build stent since presents good corrosion resistance and great availability.

Stent dimensions

Manufacturers provide a wide variety of stent sizes. Depending on the target vessel dimensions, nominal diameters generally vary from 2 to 4 mm while lengths from 8 to more the 30 mm.
As said, the nominal diameter is not the real diameter as the stent is introduced in target lesion, indeed as speaking of stent dimensions must not be forgotten the crossing profile, the strut dimension and thickness. Lower are the strut dimension and thickness, lower is the crossing profile, more easily the stent is tracked into the stenosis. Typical dimensions of coronary stent struts are in the order of magnitude of 100 μm.

There are several decisions made by the interventional cardiologist that result in a successful placement:

- Correct sizing of the stent length to match the length of the lesion, or blocked area;
- Correct sizing of the stent diameter to match the thickness of the healthy part of the artery;
- Sufficient deployment of the stent, making sure that the stent, once placed at the optimum site in the blocked artery, is expanded fully to the arterial wall. Under-expansion can, indeed, result in small gaps between the stent and arterial wall which can lead to serious problems such as blood clots, or Sub-Acute Thrombosis (SAT) while over-expansion can cause vessel ruptures with subsequent abrupt closure.

Stent design

Most of stents are made from wire or tubing. Wire stents, whose simplest shape is a coil, are used for self-expanding stents. Balloon-expandable stents are instead produced by laser cutting from tubing. The design process for stents typically involves balancing conflicting mechanical requirements. A compliant design that provides good radial support often leads to significant elastic recoil in deployment, a design that minimizes the crimped diameter often sacrifices structural strength, a stiff design that assures secure contact with the vessel may cause damage to the vessel and restenosis [20]. Trying to reach the optimal balance of strength and flexibility, different geometries have been developed, from high flexibility helical spiral, with no or minimal internal connections, passing through woven reaching the sequential rings. The latter one is the most used category and describes stent comprised of a series of expandable Z-shaped structural elements, the struts, joined by connecting elements, the bridges. This category can be further refined by describing the manner in which the structural elements are connected; distinguishing regular connection from periodic connection, open cell from close cell and peak-to-peak connection from peak-to-valley connection as explained by Stoeckel et al. [21].

Figure 2.3: *Cypher* stent from Cordis Corp.(a Johnson and Johnson Company). It is possible to see closed cells and regular peak to valley flex connectors.

Each subcategory has advantages among the others, e.g. peak to valley connection minimizes foreshortening, but open cell periodic peak to peak connection are generally used (see Figure 2.4), ensuring radial force and longitudinal flexibility.
Commercially available stent geometries are often (if not always) subjected to very strict patent claims. For this reason, manufacturer's specific and detailed information regarding the stent geometry is usually not available in the public domain. An accurate

Figure 2.4: *Element* stent from Boston Scientific Corp. Balloon expandable open cell sequential ring design with periodic peak to peak non flex connections.

geometrical representation of the stent can be acquired using a microscope or micro-Computer Tomography. The advantage of the micro-CT strategy is the possibility to build a precise three-dimensional reconstruction of both the stent and balloon directly from the CT-scans, as explained in section 2.5. The main stent dimensions can be measured and used to build a 3D CAD model of the crimped shape of the stent [16].

2.2 Finite element analysis of coronary stent

Computational studies may be used to investigate the mechanical behavior of stents and to determine the biomechanical interaction between stent and artery (e.g., the stresses caused on the vessel wall by stent deployment), but has also become an important component of the design process since gives the opportunity to evaluate which and how parameters, such material properties or design, influence the success or the failure of a simulation promoting the use of computer-based finite element analysis as a pre-clinical testing tool to analyze the biomechanical attributes of stents [22].
Such numerical studies are based on the Finite Element Method (FEM). A Finite Element Analysis (FEA) is the investigation, by numerical means, of the mechanics of

physical systems. In general, a finite element model is defined by its geometry, material properties, and some appropriate loading and boundary conditions. The continuum (e.g., a stent) is divided into a finite number of discrete regions, named elements, whose behavior can be described mathematically. An approximate solution of the entire continuum is solved from the assembly of the individual elements. The mechanical behavior (displacement, strain, stress, ...) in any point of an element is described in function of the behavior at a small number of control points (nodes) in the element. Usually, the displacements of the nodes are taken as the fundamental unknown quantities. At any other point in the element, the displacements are obtained by interpolating from the nodal displacements. The interpolation order is dependent upon the number of nodes in the element. From the displacements, the strains are evaluated by taking the appropriate derivatives. The material constitutive behavior provides the necessary basis for computing stress levels from these strains. Application of the principle of virtual work to an element yields the forces exerted by the nodes on the element, which are statically equivalent with the built-up stresses, and by Newton's third law the actions of the element on a particular node are easily found. Force contributions from all elements connected to a particular node are summed up, and must be in equilibrium with any externally applied loading or force applied to the continuum. Thus, the Finite Element Method essentially transforms the unknowns from the various continuous fields into equations of discrete nodal quantities. Assuming certain basic numerical requirements and standards of practice are satisfied, the solution obtained from the FEA estimates the exact physical solution [16].

2.3 Short review on stent deployment modeling

Computer simulation (e.g., FEA) can be a very useful tool to study and optimize the stent expansion. As accurately reviewed by De Beule [16], several stent simulations have been carried out both neglecting the presence of the balloon, by imposing a constant increasing pressure on the stent's inner surface. For further details about such numerical studies please refer to the review of De Beule [16]. Each numerical study has provided interesting and different data but most of them have highlighted the fact that the stent deploys in a non uniform manner as the balloon is neglected.

As approaching realistic stent deployment models, some key works must be kept in mind as the one of Lally et al., in 2004, who have developed a model of stenting procedure comparing two different stents, proving that different stent designs induce

different level of stress in vascular wall [22]. A finite element method computations were performed by Gijsen et al.[23] to simulate the deployment of a stent inside a 3D reconstruction of a mildly stenosed coronary artery, based on a combination of angiography and intravascular ultrasound. The method obtained can be used to predict stresses in the stent struts and the vessel wall, and thus evaluate whether a specific stent design is optimal for a specific patient [23]. The folding pattern of the balloon, and its consequent impact on uniformity on the stent expansion, has been ignored until the works of De Beule [16] and Mortier [24], who modeled stent deployment by the inflation of folded balloon. Most of the groundwork of this thesis is based on the PhD thesis of Mathieu De Beule, *Finite Element Stent Design* [16].

2.4 3D stent modeling

After understanding the main features of balloon expandable stent system, it is possible to begin the creation of a three dimensional model of a balloon expandable stent system. In order to create realistic computational models to perform simulations, the geometry of the stent and its delivery system should be very accurate. For this reason the reconstruction starts from micro-computer tomography (micro-CT) scans, a miniaturized version of computerized axial tomography (TAC), commonly used by radiologists with resolution of the order of a few micrometers. With micro-CT images the stent/balloon is partitioned in several slices and from each slice, an image is taken to achieve a sequence of images, starting from one edge of the system and ending on the other one.

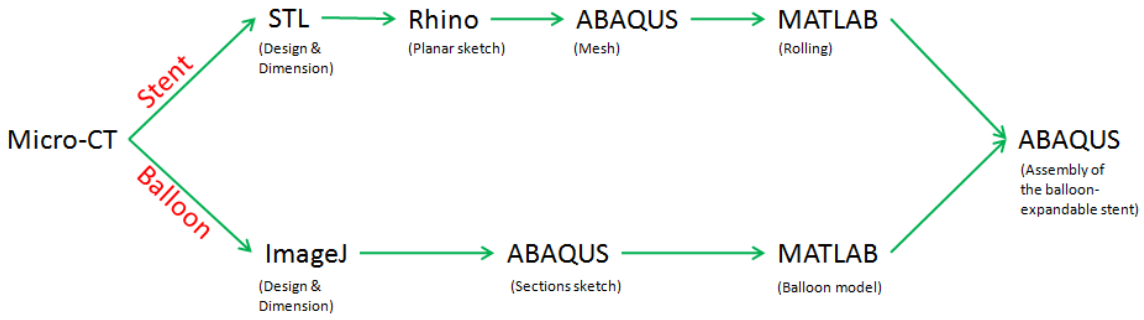

Figure 2.5: 3D reconstruction of a realistic balloon expandable stent model: process flow chart.

High-resolution stent system images, obtained with micro-CT, provide both geometry and sizes of the stent and the balloon, although the chosen post processing of these images follows two different ways: one for the balloon and one for the stent.

2.4.1 Balloon reconstruction

Balloon images have been analyzed with ImageJ, an image processing tool, to catch the diameter of the folded balloon and the exact folding pattern i.e., numbers of folding, diameter of single layers, building the folding, and angles between the folds.
Starting from one end reaching the other is not possible to analyze images of the balloon as the stent appears, since the balloon is hidden by the metallic stent struts. So, since balloon is longer than the stent, among the entire sequence of scans, has been kept the best images in the two difference sections: before and after the stent. Between the stent and the balloon end, there is a short straight segment, then the balloon decreases in diameter rotating and unfolding itself till ending in circular bases. In order to create the entire balloon, have been taken images of the straight segment, to understand the folding pattern of the balloon, and of the conical segment, to reconstruct the balloon tip.

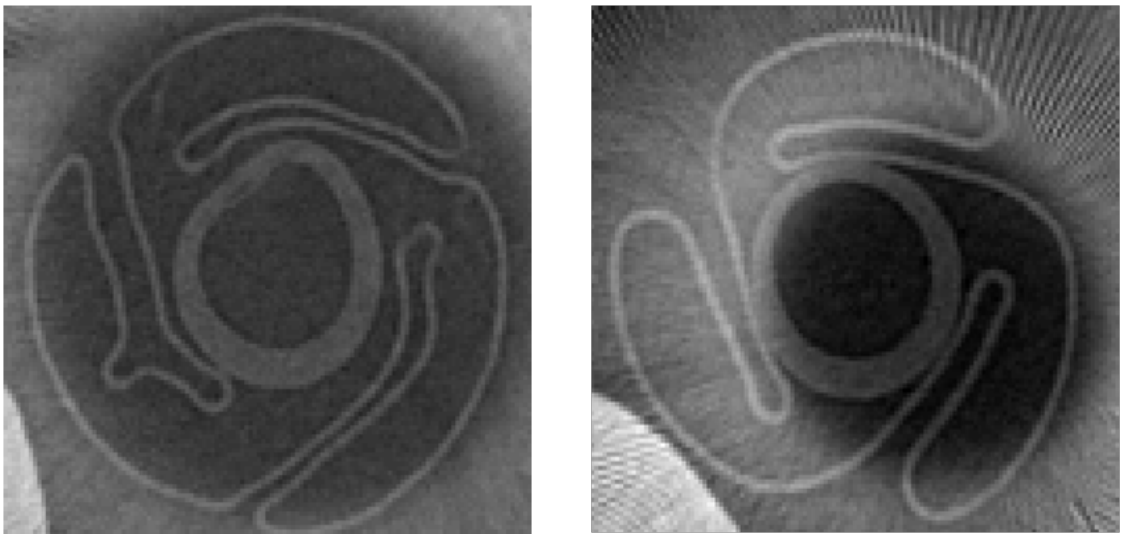

(a) Folded section. (b) Semi-folded section.

Figure 2.6: Micro-CT images of two different section of the Tryton balloon (Tryton medical,Inc., Durham, North Carolina).

Once measured sizes and features of the balloon is possible to draw the designs of

folded section and of the "semi-folded" section (a section between the folded segment and the circular end).
ABAQUS has been used to sketch these geometries. ABAQUS[2] is a powerful finite element solver, designed primarily to model the behavior of solids and structures under externally applied loading. This commercial code ABAQUS performs static and dynamic analysis and simulation on bodies with various loads, temperatures, contacts, and other boundary conditions. ABAQUS input file, an ASCII file with an extension of .inp, contains the coordinates of the nodes that builds the sketches of the balloon; so the nodal coordinates from the two ABAQUS input files have been copied and saved in a text file (.txt) and then imported on MATLAB.
MATLAB[3] is a high-level technical computing language and interactive environment for algorithm development, data visualization, data analysis, and numeric computation [25]. Through a MATLAB script, the ABAQUS files are modified, increasing numbers of nodes to obtain a design that looks like the one in the micro-CT. Increasing the nodal numbers of section, more accurately designs are implemented but longer time the simulation will take, since more element will have to be considered. A good balance between numbers of nodes and time is then desirable.

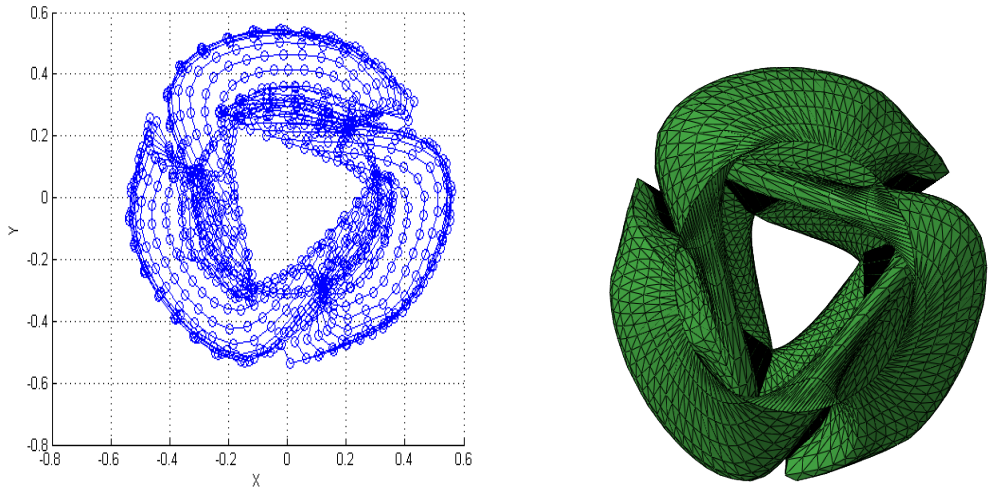

(a) MATLAB view of the balloon end.

(b) ABAQUS view of the balloon end.

Figure 2.7: X-Y views of the balloon tip reconstructed from micro-CT. From its folded configuration, the balloon rotates itself ending in circular tip.

[2]a software from SIMULIA, a Dassault Systèmes brand, Paris, France
[3]developed by MathWorks, Natick, Massachusetts USA

The cylindrical body of the balloon is built by repeating the folded section and then connecting the sections obtained. The conical balloon tapers are instead reconstructed by connecting the folded section to the semi-folded section and to a circular section created for the balloon end. Then the conical taper is sampled in a appropriate number of section to have the same distance between all the balloon sections. The entire balloon is then assembled by joining the cylindrical part and the two conical tapers.
Each section is divided into nodes and the nodes of adjacent sections are connected to create elements, thus obtaining a mesh of the entire balloon. Then an input file is written and can be brought back to ABAQUS.

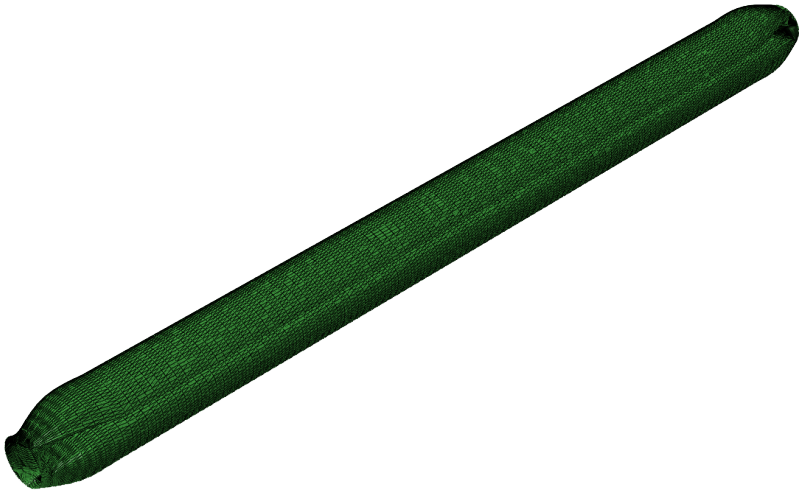

Figure 2.8: The whole reconstructed and meshed Tryton balloon (ABAQUS view).

2.4.2 Stent reconstruction

Stent reconstruction has been carried out through a different approach. Micro-CT stent images look like gear's crown wheel, so it's easy to measure inner and outer diameters and hence the strut thickness, but it is not possible to understand the stent geometry. OsiriX, an image processing software dedicated to DICOM images (.dcm extension), has a powerful 3D reconstruction tool that makes it possible to transform the micro-CT images into very accurate 3D model of the stent in a STL[4] file. STL files describe a three dimensional object whose surface geometry has been discretized into triangles.

[4] STereo Lihography

It consists of the coordinates X, Y and Z of the three vertices of each triangle, with an index to describe the orientation of the surface normal.

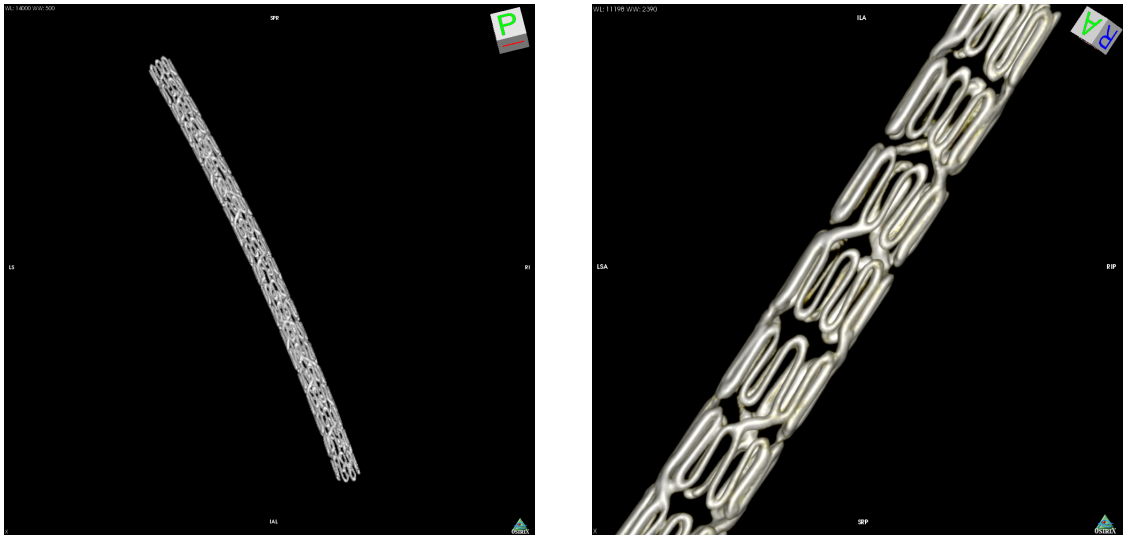

(a) Whole Element stent STL. (b) Detail view of the Element stent STL.

Figure 2.9: STL reconstruction of the Element stent by OsiriX.

As previously visualized in Figure 2.2 and here in Figure 2.9, STL file shows the design of the stent, so it is possible to measure the size and the number of struts of each ring, the number of rings, the type and size of the connectors.
Owning these parameters and using the repeating unit geometry of each stent design, solid models of the full stent can be generated. A planar geometry of the unrolled stent has been accurately drawn with Rhinoceros 4.0 (from McNeel&Associates, Indianapolis, USA), a NURBS[5]-based 3D modeling tool used for industrial design. The solid models generated are the ones of the stents in a planar state, i.e., the geometry of the stents if they were cut open longitudinally and flattened out.
The stent solid model has then been imported and meshed in ABAQUS. Once the stent has been meshed, the nodal coordinates from the ABAQUS input file have been copied and saved in a text file and then imported on MATLAB, as done for the balloon. The stent has then to be wrapped into a cylindrical shape by transferring the nodal coordinates from a cartesian coordinate system into a cylindrical coordinate system.
Therefore another MATLAB script has been implemented to roll the stent, giving stent radius, length and the text file containing the nodal coordinates and receiving an input

[5]Non-Uniform Rational B-Splines i.e., mathematical representations of 3D geometry able to represent most of the 3D organic free-form surface or solid

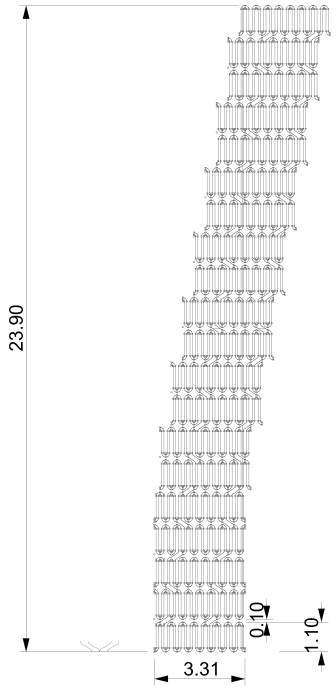

(a) Planar sketch of the Element stent from Rhinoceros

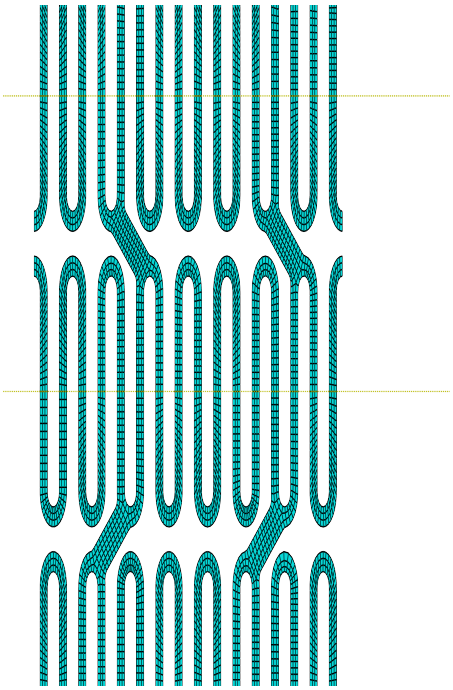

(b) Detail of the planar mesh of the Element stent from ABAQUS

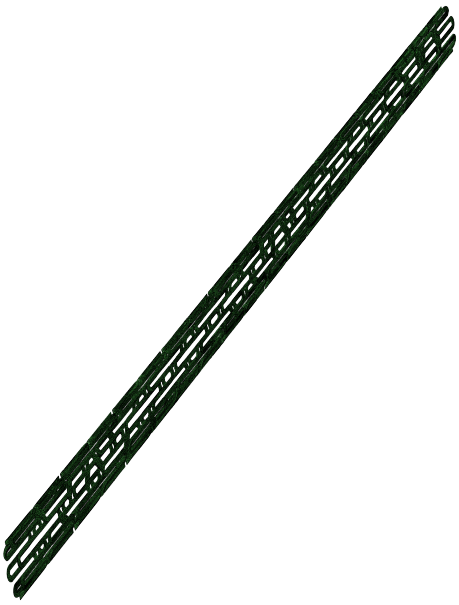

(c) Entire meshed stent

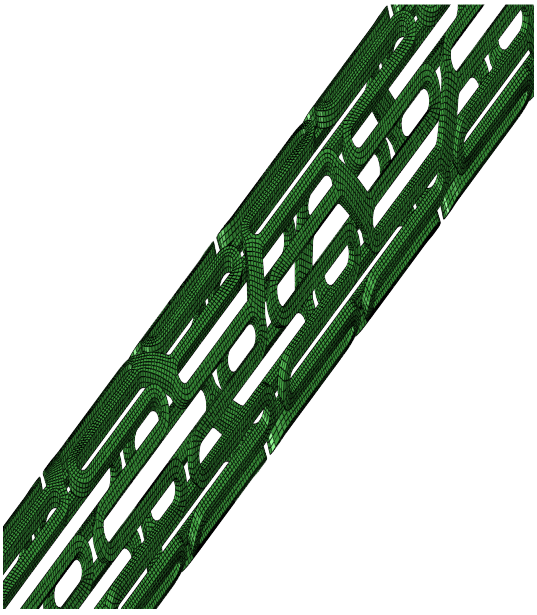

(d) Zoom of the stent mesh

Figure 2.10: Reconstruction of the Element stent

file ready to be imported in ABAQUS. In this way FE meshes were generated for each stent design as shown in Figure 2.10.
Once the balloon and the stent have been reconstructed, most of the work has substantially been done since the next step consists of assembling the two parts just created.

2.5 Creation of a stent library

Each stent and each balloon are provided by manufacturer in a wide variety of sizes. Once reconstructed the design of the balloon and the stent, it's possible to resize it to create a library of stent and balloon, i.e., different stent lengths can be obtained adding or removing rings while diameters can be varied by rescaling the inner and the outer diameter since the strut thickness remains the same.
Having a balloon and stent library, different analysis can be perfomed not only to compare different stent design and outcomes, but most important to better choose which stent and which balloon is perfectly suitable for a specific stenosic artery. A possible implementation of the stent library is visualized in Table 2.2.

Stent System		**Manufacturer**	**Design**	**Materials**	**Size (Nominal diameter x nominal length) [mm]**
Cypher sirolimus-eluting coronary stent	Raptor balloon	Cordis Corp.	3-folded	Duralyn	13.5 x 3.0
	Cypher stent			316L stainless steel	8.0 x 3.0 10.0 x 3.0
Element stent	...	...	...	...	...
				...	...

Table 2.2: Example of a stent library.

2.6 Conclusions

In this chapter the key characteristics of the stent delivery system have been presented in order to have a wide overview of how this structure is made of and how it works. Achieved this basic knowledge, it is possible to create a model to investigate the mechanical behavior of the stents. Numerical studies, based on the Finite Element Method, offer numerous possibilities in the optimization of coronary stenting procedure. The development of a virtual framework to study the mechanics of stents, in a variety of materials, seems to be an interesting challenge. Such a modeling tool should be able to accurately predict the most important stent characteristics (e.g. expansion, recoil, dogboning, foreshortening, flexibility, stiffness, etc.).

The reconstruction of realistic stent models staring from micro-CT images, as explained, paves the way to the evaluation and comparison of different models of the free expansion of a balloon expandable stent and can be easily applied to most coronary stent designs.

Chapter 3

Balloon expandable stent deployment

The growing number of available stents increases the freedom for the physicians to choose, but it also brings along the question of which stent to use for which particular case/type of stenosis. For example, a very flexible stent with a low crossing profile may be required to treat patients with highly tortuous vessels. Therefore, objective comparisons of these stents are needed in terms of geometrical aspects of the design and mechanical performance among many others, because all of these parameters are important for optimal stent selection.
Finite element studies are ideal to compare the mechanical behavior of different stents. Such analysis provide several informations, as stresses on the stent and on the arterial walls, and allow virtual investigation of different design parameters without the need to manufacture prototypes until an optimal design has been identified.
Using finite element simulations to study coronary stents deployment is not trivial. All the individual components (balloon, stent, stenosis) have a complex geometry, undergo large deformations and also interact with each other. For these reasons, it is important to go step by step instead of immediately jumping to full scale stenting simulations. This chapter begins with a realistic and validated model of the expansion of a folded angioplasty balloon based on the manufacturer's compliance chart. Subsequently, is presented a realistic model of a coronary stent expansion, driven by balloon inflation.

3.1 Balloon expansion modeling

Several numerical studies of expansion of balloon expandable coronary stents have been carried out, following three scenarios: (i) ignoring the balloon and applying an increasing uniform pressure directly on the stent inner surface, (ii) accounting for balloon-stent interaction and enforcing a radial displacement-driven process on a cylindrical balloon and (iii) accounting for balloon-stent interaction by applying an increasingly uniform pressure on the inner surface of a trifolded balloon. Neglecting the folding pattern alters the stent expansion, since has been proved that the length and the folded shape of the balloon influences the uniformity of stent strut distribution [16]. In order to create a realistic three dimensional model of balloon expandable stent deployment, the balloon design has to be considered.
In the studies done by De Beule [16] and Mortier [24], the balloon ends were discarded from the model. Creating a balloon model taking into account both the folding pattern and the balloon ends, is the aim of this section.

3.1.1 Introduction

The noncompliant Sprinter balloon[1] has been chosen for simulate the balloon inflation. The Sprinter balloon is an angioplasty balloon commercially available in more than 60 sizes and different folding pattern. A model of this balloon has been developed and different simulations have been carried out to analyze its behavior.

3.1.2 Material and methods

Model geometry

The free expansion of the Sprinter balloon is simulated and validated through the comparison with the manufacturer's compliance chart. The Sprinter balloon chosen for the simulations implemented has a nominal diameter and a nominal length of 3 mm and 15 mm, respectively.
The Sprinter compliance chart is given by manufacturer in a pressure range varying from 0.8 N/mm^2 (8 atm) to 2.2 N/mm^2 (22 atm), but the balloon must not exceed pressures higher than the Rated burst pressure of 1.8 N/mm^2 (i.e, the maximum pressure to which the balloon is designed to be inflated).
The Sprinter's compliance chart is presented in Figure 3.1.

[1] from Medtronic, Inc., Minneapolis, Minnesota

Pressure (atm)	Balloon Diameter (mm)										
	2.00	**2.25**	**2.50**	**2.75**	**3.00**	**3.25**	**3.50**	**3.75**	**4.00**	**4.50**	**5.00**
8	1.98	2.17	2.45	2.70	2.97	3.09	3.36	3.62	3.87	4.27	4.75
9	2.00	2.20	2.49	2.74	3.01	3.15	3.42	3.68	3.93	4.34	4.84
10	2.02	2.23	2.51	2.77	3.04	3.18	3.45	3.72	3.97	4.39	4.91
11	2.03	2.24	2.53	2.80	3.07	3.22	3.49	3.76	4.01	4.44	4.97
12	2.05	2.26	2.55	2.82	3.10	3.25	3.52	3.79	4.05	4.48	5.01
13	2.07	2.28	2.57	2.84	3.13	3.28	3.55	3.82	4.08	4.51	5.06
14	2.08	2.30	2.58	2.87	3.15	3.31	3.58	3.85	4.11	4.55	5.10
15	2.10	2.32	2.60	2.89	3.18	3.33	3.61	3.88	4.15	4.58	5.14
16	2.12	2.33	2.62	2.91	3.20	3.36	3.63	3.90	4.18	4.61	5.18
17	2.13	2.36	2.63	2.93	3.23	3.39	3.65	3.93	4.22	4.65	5.22
18	2.15	2.38	2.65	2.95	3.26	3.41	3.68	3.96	4.25	4.68	5.26
19	2.17	2.40	2.66	2.98	3.29	3.44	3.71	3.99	4.29	4.72	5.30
20	2.19	2.42	2.68	3.00	-	3.47	3.73	4.02	-	4.76	-
21	2.21	2.44	2.70	3.03	-	3.50	3.77	4.05	-	4.80	-
22	2.23	2.46	2.72	3.05	-	3.53	-	4.08	-	4.84	-

Figure 3.1: Compliance Chart of the Sprinter Balloon from Medtronic, Inc. [26]. Light blue line: Nominal pressure, Green line: Rated burst pressure.

Interpolating the compliance chart values of the interested diameter with a linear curve, and projecting the line achieved to the diameter axis, it has been obtained an initial diameter of 2.765 mm at zero pressure. The initial diameter achieved is then used to scale the balloon sketch. The number of folds of the noncompliant Sprinter balloon varies with its diameter. Balloons, whose diameter are higher than 3.75 mm, present a five-folded disegn whereas balloons with smaller diameter have the classical trifolded configuration, so the model developed is a trifolded balloon. Despite the awareness of the number of folds, the realistic folding pattern and folded diameter have been unknown. It has been therefore created an idealized sketch of the trifolded balloon shape using the graphical finite element preprocessor ABAQUS/CAE. The design of the Sprinter balloon folding pattern, is depicted on the left in the Figure 3.2.

Since the diameters of the folded geometry were not available, the balloon folded sketch has been created without any measures but through a MATLAB script, the entire design has been scaled. After having calculated the length of the balloon sketch and derived its unfolded diameter, each node of the section has been scaled achieving a folded diameter of 0.78 mm.

The balloon folded pattern has to rotate and partially unfold in order to reach its circular ends, whose diameter is assumed to be 0.6 mm. In order to connect the folded part with the circular extremity, another sketch has been drawn.
Figure 3.2 shows the semi-folded sketch (right).

(a) Trifolded balloon section.

(b) Semi-folded balloon section.

Figure 3.2: ABAQUS sketches of the Raptor Balloon. The straight body of the balloon has a trifolded pattern (left), while close to its ends, the balloon rotates and partially unfolds in a semi-folded configuration.

The connection between folded section, semi-folded section and circular section is not trivial since intersections can occur thus hindering the balloon deployment. Therefore the circular section and the semi-folded section have been accurately rotated to avoid intersections but also to achieve the maximum internal lumen in order to insert the catheter and the guide wire. As done for the folded sketch, the semi-folded sketch has been scaled. In Figure 3.3 are depicted the scaled sections of the balloon.

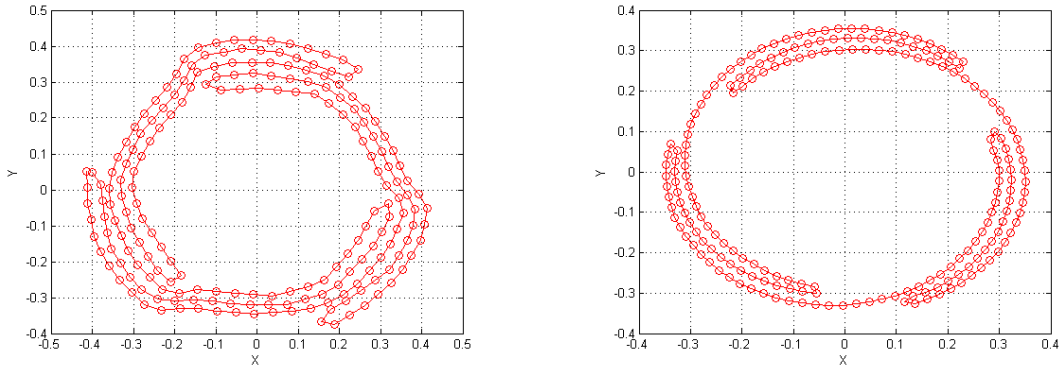

(a) Trifolded balloon section.

(b) Semi-folded balloon section.

Figure 3.3: Matlab section of the Sprinter Balloon resulting from ABAQUS sketches.

The length of the non-tapered cylindrical part is 12 mm, while the complete balloon measures 15mm from proximal to distal balloon tip and the uniform balloon thickness is considered to be 0.02 mm.

Material properties

The semi-compliant Raptor balloon is fabricated from Duralyn, a nylon-based material. The constitutive behavior of this material is described by the compliance chart of the balloon, provided by the manufacturer. The methodology used to deduce the constitutive law of the balloon from the compliance chart is based on the thin shell membrane theory and results in stress/strain data [16]. A Matlab script has been therefore implemented to calculate the Young's modulus of the material from the pressure/diameter data, resulting in 920 N/mm^2. In addition, the balloon material is characterized by a Poisson's ratio of 0.4 and a density of 1100 g/cm^3.

Numerical aspects

The balloon has been meshed in MATLAB with 3-node triangular membrane elements (M3D3). It has been chosen triangular elements instead of quadrilateral in order to have a larger number of node for each section without having intersections as the balloon decreases in diameter. Each section was composed by 180 nodes resulting in 35280 elements. In order to prevent the inertial forces to alter the dynamics of the expansion, a smooth step load has been chosen.
A rising pressure, starting from zero reaching the rated burst pressure of 1.8 N/mm^2, has been applied on the inner surface of the balloon. The balloon has been constrained at both ends thus avoiding its movement and shortening during the inflation. The boundary conditions and the load applied to the balloon are depicted in Figure 3.4.

Finite element simulations

The stent expansion would be study with a static approach since the target of the stent modeling is to analyze the equilibrium of the stent delivery system. Proceeding with a static analysis, some non linearities been have encountered due to the material, the large deformations and contact problems leading to a problematic convergence and difficulties in defining a generic approach.
In order to overcome such problems, especially the contact problems, the explicit solution method has been preferred to the static analysis. Indeed all the stent expansion

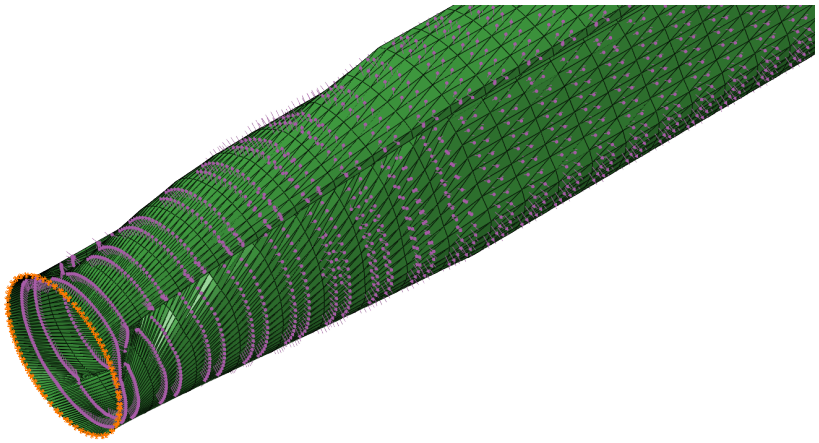

Figure 3.4: Loads and Boundary conditions applied to a portion of the Sprinter balloon.

simulations were carried out using the ABAQUS/ EXPLICIT solver.
Applying the explicit dynamic procedure to quasi-static problems, as the stent deployment, requires a very small time increments and leads to the presence of inertial forces, which should be kept as small as possible. Such problems lead to an high computational cost. In order to reduce the time increment without altering the analysis. So the time period of the quasi-static stent expansion process has been decreased with the aim of reducing the computational time. The main problem is that as the expansion is accelerated, the presence of inertial forces may become dominant and modify the response of the system. In this work, to follow a cost-saving approach maintaining solution accuracy, an element-by-element stable time increment estimate coupled with a variable mass scaling technique was used, allowing an ad hoc adjustment of the material density in space and simulation time. Analysis time-step and loading rate were adequate to ensure a static equilibrium along the analysis.
Complex contact problems appear as the balloon deploys since the folds interact each other. The general contact algorithm has been used in order to handle these interactions, the frictional behavior has been described by a Coulomb friction model with a static friction coefficient of 0.2 (valid for a nylon-nylon and a nylon-steel friction couple under clean conditions). These contact specifications allow avoiding numerical instabilities in the simulation of the interactions [16].

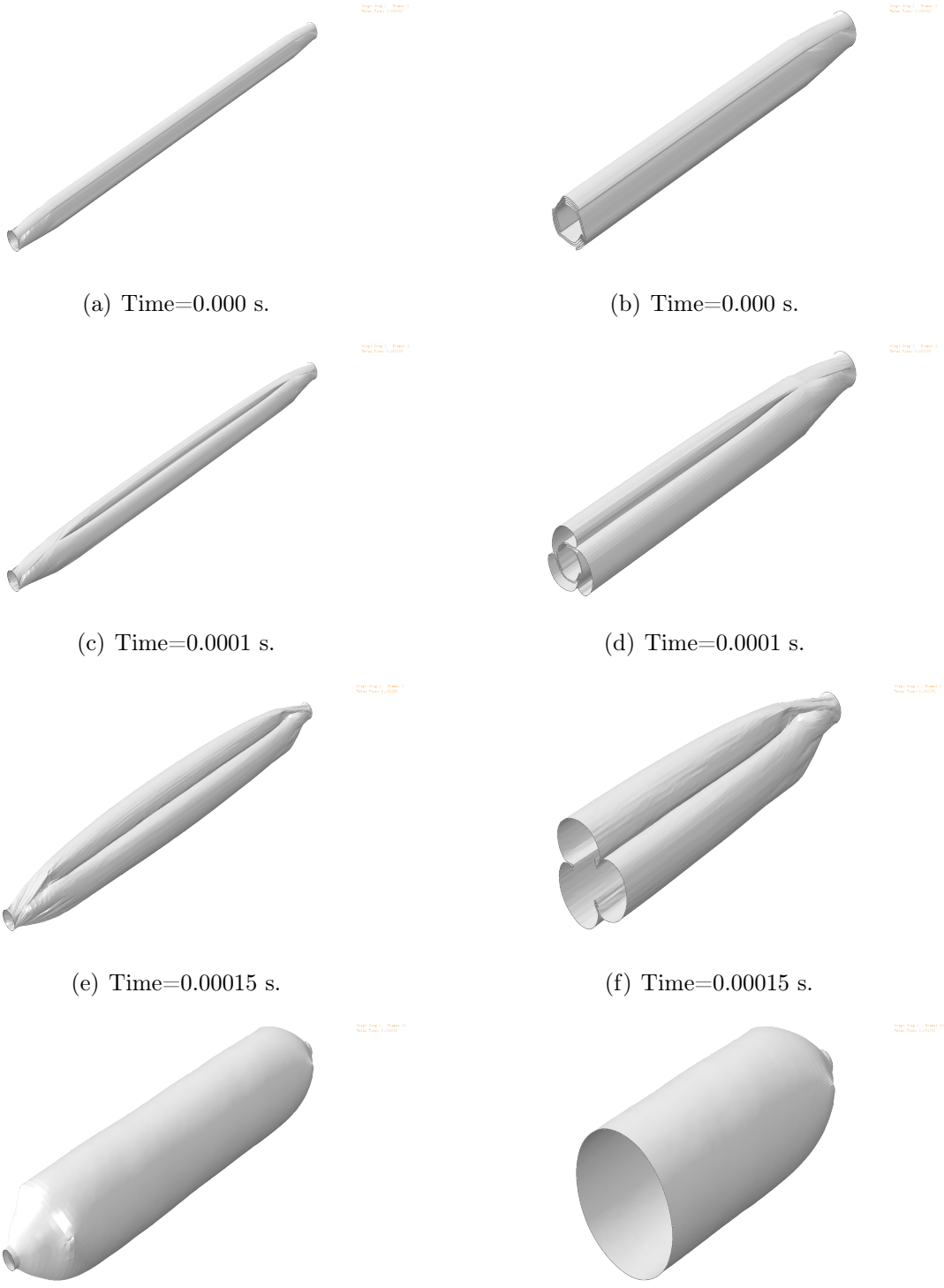

(a) Time=0.000 s.

(b) Time=0.000 s.

(c) Time=0.0001 s.

(d) Time=0.0001 s.

(e) Time=0.00015 s.

(f) Time=0.00015 s.

(g) Time=0.001 s.

(h) Time=0.001 s.

Figure 3.5: The Sprinter Balloon unfolding; left panel: the entire balloon view, right panel: cross sectional view. From the top to the bottom can be seen different steps of the inflation.

3.1.3 Results and discussion

The Sprinter balloon unfolding process is depicted in Figure 3.4. A very close agreement in compliance between the results from both analysis and data provided by the manufacturer reveals the potential of the proposed approach. The expansion of the folded angioplasty Sprinter balloon is characterized by a rapid unfolding at low pressure followed by an increase of diameter of the cylindrical shape at higher pressures, as confirmed by data graphically represented in the left panel of Figure 3.7. The results of the simulations in terms of pressure and balloon diameter are summarize in Figure 3.6.

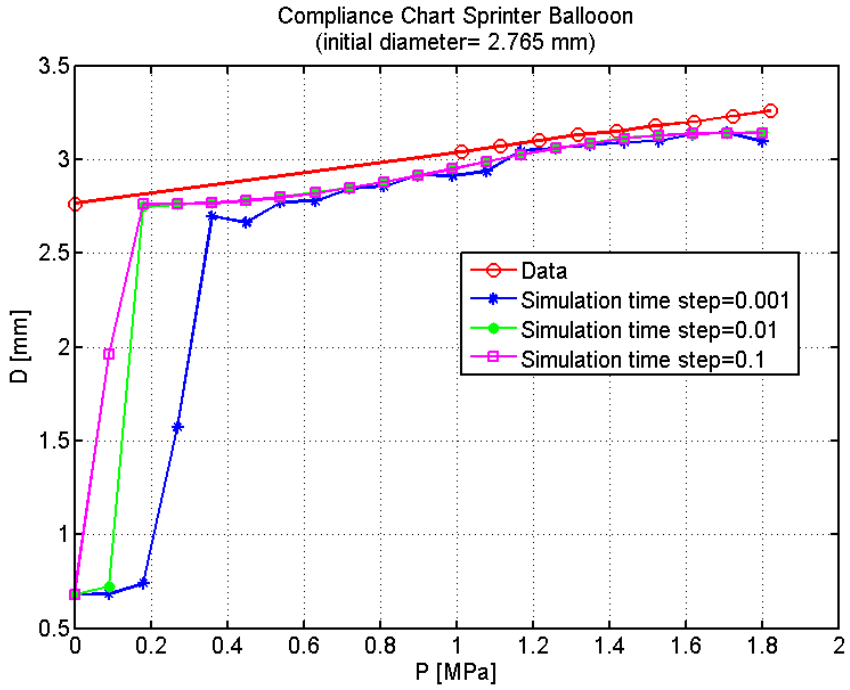

Figure 3.6: Compliance chart of the Sprinter Balloon. Simulations with different step time has been carried out to highlight the behavior of the balloon.

Different simulation time steps have been implemented; as the simulation time increases, the compliance chart obtained follows more accurately the data provided by the manufacturer. The initial difference between the data provided by manufacturer and all the simulations was due to the unfolding process since the compliance chart data given by Medtronic, Inc. already refers to the balloon cylindrical shape. The percentage error between the simulation and manufacturer data, shown in the right

panel of Figure 3.7, has remained lower than 5% in all the simulations.

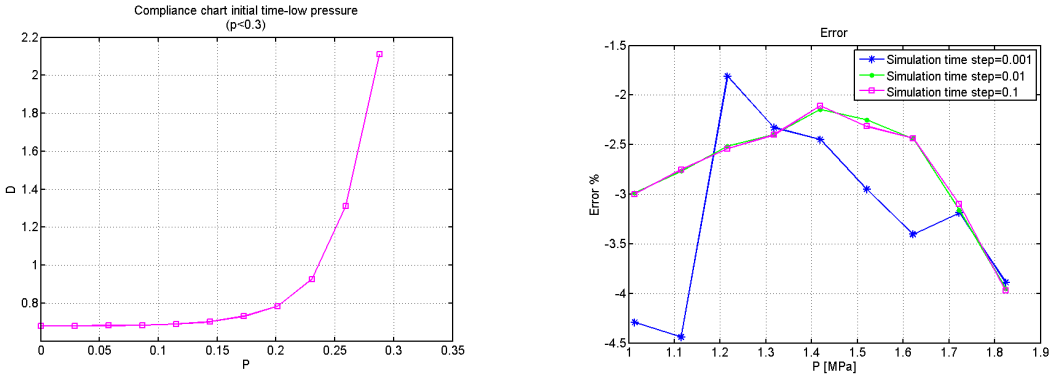

(a) Initial trend of the compliance chart obtained with a simulation time of 0.1 s.

(b) Percentage error between the simulation and manufacturer data.

Figure 3.7: Postprocessing analysis.

Limitations

Despite the realistic results, some limitations have to be taken into account. No micro-CT scans and no data regarding the balloon thickness were available, so the geometry of the noncompliant Sprinter balloon has been reconstructed as idealizing the folding pattern. One way to overcome these limitations is to directly use micro-CT based 3D reconstruction through the procedure previously explained in section 2.4. Moreover the simulation time has been reduced since, using the realistic inflation period, would have required an excessive computational cost. Furthermore, in clinical practice the balloon is expanded by inserting a certain volume of liquid inside, while in this case the balloon has been inflated by applying an uniform rising pressure on its inner surface.

3.1.4 Conclusions

The folded balloon methodology presented here, shows very good quantitative and qualitative agreement with respectively manufacturer's data.
Based solely on the manufacturer compliance chart, it has been created a unique MATLAB script to reconstructed entire 3D models of different angioplasty balloons expansion. Despite limitations in the geometrical design of the balloon, optimal results have been reached. Therefore, the proposed numerical expansion strategy appears to be a very promising optimization methodology in stent design.

3.2 Stent expansion modeling

3.2.1 Introduction

In this paragraph a three-dimensional stent model of the *Cypher* sirolimus-eluting coronary stent[2] has been created. The commercially available Cypher coronary stent is crimped on a *Raptor* balloon, which is trifolded around the cylindrical catheter tube. The catheter tube and the tips were included in the model as they interact with the balloon during the unfolding process.

3.2.2 Material and methods

A finite element model is defined by its geometry, material properties and some specific numerical aspects (e.g. appropriate loading and boundary conditions). To simulate the free expansion of balloon expandable stents, these prerequisites are described below.

Balloon geometry

As stated in Chapter 2, the procedure to obtain the balloon sizes and folding pattern starts from micro-CT images. Unfortunately micro-CT images of the *Raptor* balloon were not available. It has been therefore created an idealized trifolded shape using the graphical finite element preprocessor ABAQUS/CAE. Based on the methodology previously implemented 3.1.3, the balloon folding pattern has been drawn and then resized achieving a folded diameter of 0.78 mm in balloon straight body, which decreases to 0.6 mm on the balloon circular end. The length of the non-tapered cylindrical part is 10.5 mm, while the complete balloon measures 13.5 mm from proximal to distal balloon tip and the uniform balloon thickness is considered to be 0.02 mm.

Stent geometry

The Cypher geometry has been downloaded from the Stent Research Unit website of University of Ghent [27]. This coronary stent has a nominal length of 8 mm and a nominal diameter of 3 mm. The inner and outer diameter of the crimped stent are 0.85 mm and 1.15mm respectively, resulting in 0.15 mm (0.0055") of thickness as provided by the manufacturer. The length of the crimped stent is 8.4 mm so that, once placed the stent on the balloon, the balloon straight part exceeds the stent of 1 mm in length at both stent ends.

[2]Cordis, Johnson&Johnson, Warren, NJ

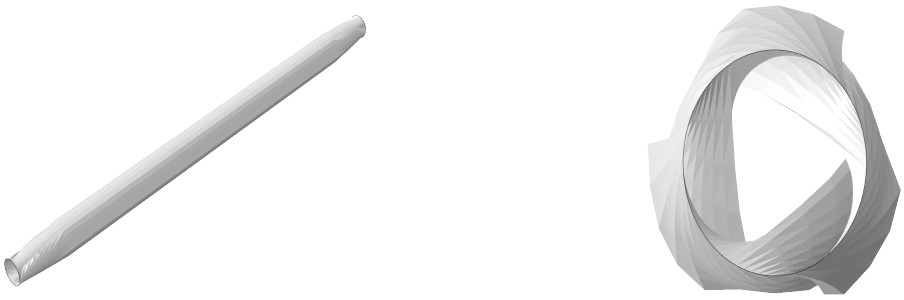

(a) Entire balloon. (b) Cross-sectional view of the balloon.

Figure 3.8: The Raptor balloon model reconstructed in ABAQUS.

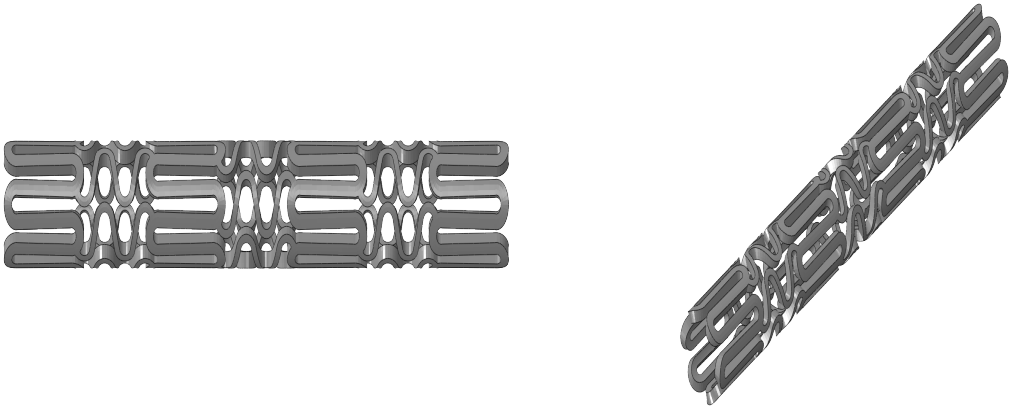

Figure 3.9: The Cypher stent model reconstructed in ABAQUS.

Tips, Catheter and Guide wire geometry

As stated in Chapter 2, the angioplasty balloons are capped with two short tubular tips, whose length is assumed to be 1 mm and inner diameter is 0.28 mm, the same as the diameter of the catheter tube, since they are connected. The cylindrical tip outer diameter measures as the balloon end diameter, i.e., 0.6 mm. The conical tip outer diameter, instead, decreases from the balloon end diameter to 0.36 mm.
The catheter shaft is a tube placed inside the balloon connected with the two tips so its length is 13.5 mm, the same as the balloon length, and its diameter is 0.28 mm, as tips diameter. The guide wire is modeled as a cylinder running through the catheter and the tips i.e., the catheter shaft, acting as the track for the movement of the entire stent/balloon device. The diameter and length of the guide wire are assumed to be 0.13 mm and 17.5 mm, respectively.

Material properties

The semi-compliant Raptor balloon is fabricated from Duralyn, a nylon-based material. As done for the Sprinter balloon, through a MATALB script, the constitutive behavior of this material has been achieved. The material is characterized by a Young's modulus of 920 N/mm^2, a Poisson's ratio of 0.4 and a density of 1100 g/cm^3.
The balloon expandable Cypher stent is manufactured in 316L stainless steel. The inelastic constitutive response is described through a von Mises plasticity model with isotropic hardening. The Young's modulus, the Poisson's ratio, the yield stress and the density are 196000 N/mm^2, 0.3, 375 N/mm^2 and 7800 g/cm^3, respectively [24].
The catheter tube and the tips are, instead, characterized by a linear elastic material with a Young's modulus of 1000 MPa, a Poisson's ratio of 0.4 and density of 940 kg/m^3, since contain high density of polyethylene components [28].
Finally the guide wire is considered to be made only by Nitinol so the Young's modulus, the Poisson's ratio and the density are 35780 N/mm^2, 0.4 and 6450 g/cm^3, respectively.

Boundary conditions and Loads

To simulate the free expansion of the stent has been applied an increasing uniform pressure starting from 0 N/ mm^2 up to 1.5 N/ mm^2 on the inner surface of the tri-folded balloon.
Both ends of the balloon have been tied with tips extremities in order to prevent the balloon movement but allowing its expansion. Boundary condition has been then applied to both the tips. All the translational degrees of freedom have been constrained on the proximal face of the cylindrical tip and on the distal face of the conical tip thus preventing the movement and the shortening of the balloon. Catheter and tips have been also tied together to create the catheter shaft, the passageway within which lays the guide wire.
In order to avoid rigid body motion of the stent, six central nodes lying in the mid-section are constrained z-direction of the cylindrical coordinate system placed in the center of the proximal face of the cylindrical tip. Guide wire has also been bounded in distal and proximal surface to avoid its movement.

Discretization

The stent has been meshed with three-dimensional 8-node brick 'reduced-integration' elements (C3D8R) using ABAQUS finite element code. To keep the analysis run-time reasonable, a finite element mesh consisting of 17280 elements was used for the Cypher stent. The trifolded balloon mesh consists of 14080 (M3D3) 3-node triangular membrane elements. The MATLAB script, developed for the balloon creation, provides an additional tool to mesh the balloon in which it is possible to choose between 4-node quadrilateral or 3-node triangular elements. The catheter tube was modeled with four-node doubly curved thin or thick shell, reduced integration elements (S4R). Both the cylindrical and the conical tips have been meshed with 1600 C3D8R elements, the same as the stent. Also the guide wire mesh consist in 8-node brick 'reduced-integration' elements, but only 480 elements has been required since in this case a large number of elements has not been necessary, further in this work more finer mesh of the guide wire will be applied. Parts of the meshed stenting device are visualized in Figure 3.10.

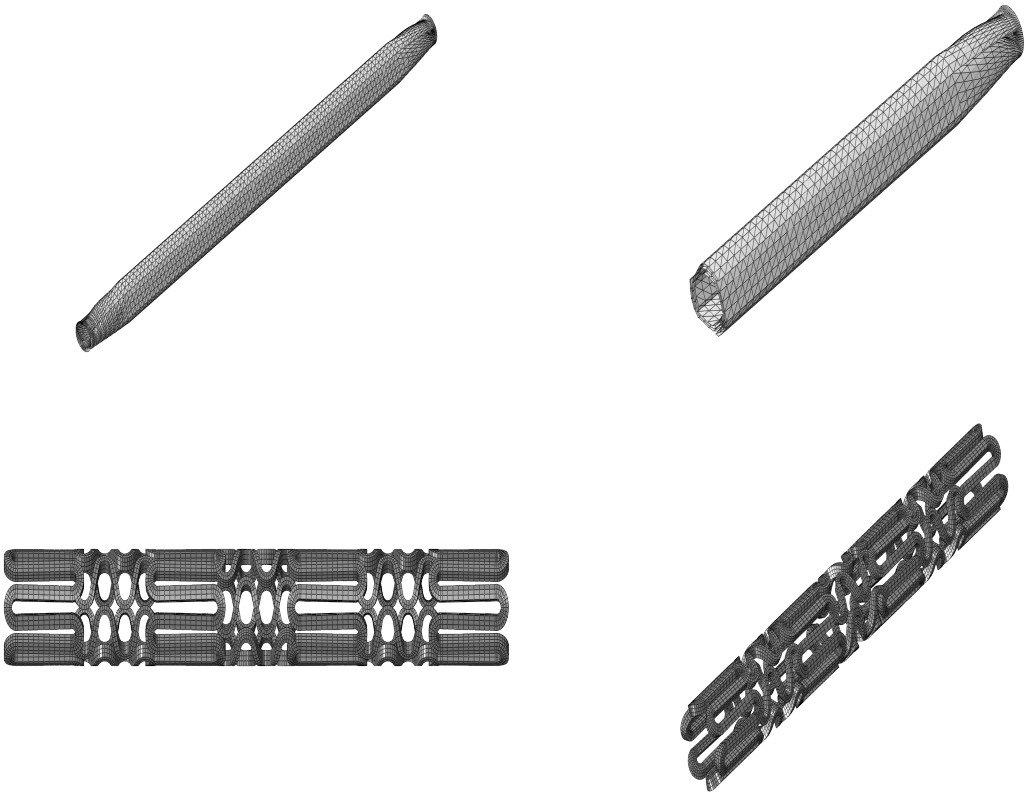

Figure 3.10: The Raptor balloon and the Cypher stent meshes.

Finite element simulations

The key features of the analysis performed are the presence of non-linearities, due to large deformations and (self) complex (self-)contact problem. ABAQUS/Explicit proved perfectly suited for the solution of quasi-static problems, especially those involving extremely complex contact conditions, as the balloon inflation procedure. The general contact algorithm has been used in order to handle the interactions between all the stent stìystem parts, as the balloon interacts with the catheter, the tips, the balloon-itself and the stent and the guide wire interacts with the catheter and the tips. Friction has been included in the simulations by means of a Coulomb friction model with a static friction coefficient of 0.2. The time period of the quasi-static stent expansion process has been decreased with the aim of reducing the computational time. The main problem is that as the event is accelerated, the presence of inertial forces may modify the response of the system. Internal and kinetic energies were monitored during the stent expansion in order to assure that the inertial forces were acceptable. As shown in Figure 3.11 during most of the expansion process, the ratio between kinetic and internal energy of the whole model was lower than 5% (i.e., under the range recommended by ABAQUS), verifying the quasi-static regime hypothesis. Only during the initial transition period between the crimped and the expanded state the ratio was higher.

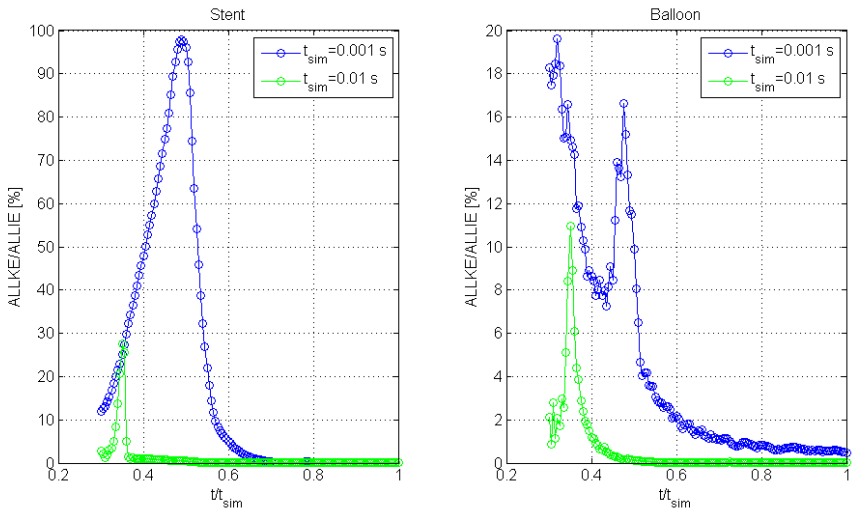

Figure 3.11: Ratio between the kinetic energy (ALLKE) and the internal energy (ALLKE) for the Cypher stent and the Raptor balloon.

3.2.3 Results and discussion

Simulation results

The Figure 3.12 shows the stent deployment patterns prior to, during and after the transient expansion phase. The expansion has asymmetrically pattern, as can be visualized in the Figure 3.11, due to a small positioning inaccuracies. Indeed the stent end corresponding with the longest free balloon end opens first, because at that end, the same pressure acts on a larger balloon surface, as explained by De Beule [16]. These results can be validated though comparison with data provided by the manufacturer.

Limitations

As the stent deployment simulations shows encouraging results, it must be recognized some limitations in the proposed approach. These limitations primarily pertain to the balloon and stent geometry, since the stent and the balloon have not been reconstructed by micro-CT images. Indeed, the stent was imported from the De Beule's work while the balloon geometry has been idealized. Furthermore, the use of a static friction coefficient to describe the interaction between the distinct parts of the stent delivery system is a simplification of reality. A dynamic friction coefficient would probably be a better approximation of reality [16].

Conclusions

The proposed stent modeling strategy incorporates the folding pattern of the balloon. This approach provides designers the possibility, not only to focus on the global behavior of the stent but also to examine the effect of the folding pattern of the balloon on the stent expansion behavior, resulting in a more realistic model of the stenting procedure.

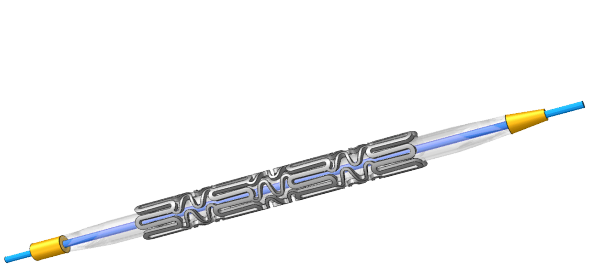

(a) Time=0.000 s.

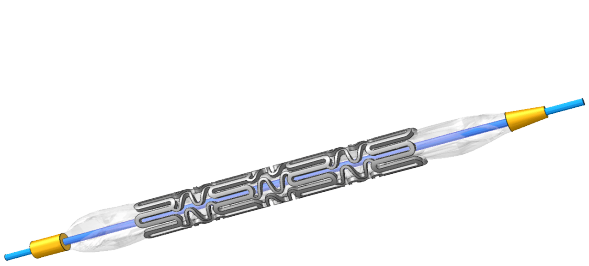

(b) Time=0.003 s.

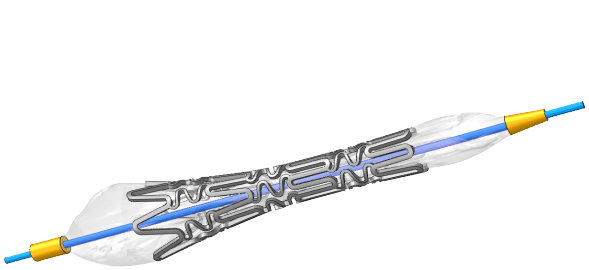

(c) Time=0.0035 s.

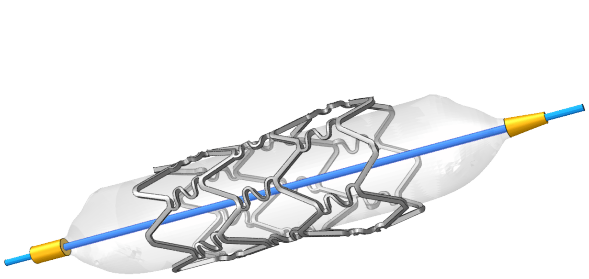

(d) Time=0.01 s.

Figure 3.12: The Cypher stent expansion. From the top to the bottom can be seen different steps of the stent deployment.

3.3 Conclusions

This study supports the use of computer-based finite-element analysis as a pre-clinical testing methodology to analysis the biomechanical attributes of balloon expandable stents. The proposed virtual design space has the potential to significantly speed-up the design phase and to provide physicians with additional information to compare different designs (from different manufacturers) in an objective manner. It can be concluded that:

- The proposed methodology to simulate the free expansion of folded angioplasty balloons allows to determine approximate balloon material properties and appropriate boundary conditions (which mimic the balloon tapering) based solely on the manufacturer's compliance chart. Through an unique MATLAB script is possible to create different balloon models from every manufacturer. The numerical results in terms of pressure and diameter show very good agreement with data provided by the manufacturer and consequently the proposed balloon model seems a valuable tool to study realistic balloon/stent interactions.

- Using the proposed trifolded balloon methodology seems to great advantage, since the free expansion of a stent is governed by the unfolding and expanding of the balloon. Moreover, the trifolded balloon expansion methodology shows very good quantitative and qualitative agreement with manufacturer data.

- Changing the balloon length and folding pattern can have an enormous influence on the transient stent expansion behavior. Therefore, the proposed methodology can be used to select the most appropriate balloon length and folding pattern for a particular stent design.

The absence of the artery in the models, just described, leads to an incomplete understanding of the stent system deployment. Numerical models developed in Chapter 4 will incorporate the artery and this will allow to study the resulting stresses in the vessel wall.

Chapter 4

Stent insertion and deployment in a coronary artery

The stenting procedure has the goal to widen an occluded artery. Simulating solely the deployment of balloon expandable stent system provides some interesting information but for the physician's choice between different stent typologies, the merely deployment without the presence of the stenosed vessel can result useless.
Numerous computational studies have been carried out to investigate the expansion and mechanical behavior of different stent designs. However, very few analysis have been performed on the interaction between the stent and the artery. The stress state and the associated injury induced by stent placement are, instead, important factors to consider as they were identified as contributors to the complex reaction processes that lead to restenosis 1.5. An ideal stent design should, therefore, avoid tissue damage as much as possible and minimize the induced stresses, while providing sufficient radial support.
In this chapter, a simulation strategy considering the insertion of a folded balloon catheter over a guide wire is proposed in order to position the stent within the straight and curved vessel. Furthermore the deployment of two other stents is simulated.

4.1 Stent insertion and deployment in a straight coronary artery segment

4.1.1 Introduction

The stenting procedure consists in five different steps:

- Guide wire insertion
- Stent/balloon movement over the guide wire
- Balloon inflation and following stent deployment
- Balloon deflation
- Balloon and guide wire removal

In the methodology developed in this chapter the first and the last steps have been ignored in order to focus only on the stent insertion and deployment. The balloon deflation, instead, has to be taken into account since provides additional information such as the radial strength of the stent under the elastic recoil of the vessel walls.
The balloon expandable Cypher stent has been chosen for the insertion and deployment in a coronary artery.

4.1.2 Materials and Methods

A finite-element analysis requires the geometry and material properties of the stent and blood vessel and appropriate loading conditions to simulate the stenting procedure, as described below.

Stent/balloon model

The same geometry, designs and materials implemented in the previous Chapter to simulate the Cypher deployment has been used. So the model assembled has been copied in a new ABAQUS file. Only the guide wire has been modified. In Chapter 3, indeed, the guide wire has been included to create a realistic model of the stent system but has been functionless. While modeling the stent insertion, instead, the guide wire acts as a determining instance of the delivery system since it represents the rail on which the balloon/stent travels. The guide wire developed is 40 mm long and has a diameter of 0.1 mm. The whole stent/balloon model is visualized in Figure 4.1.

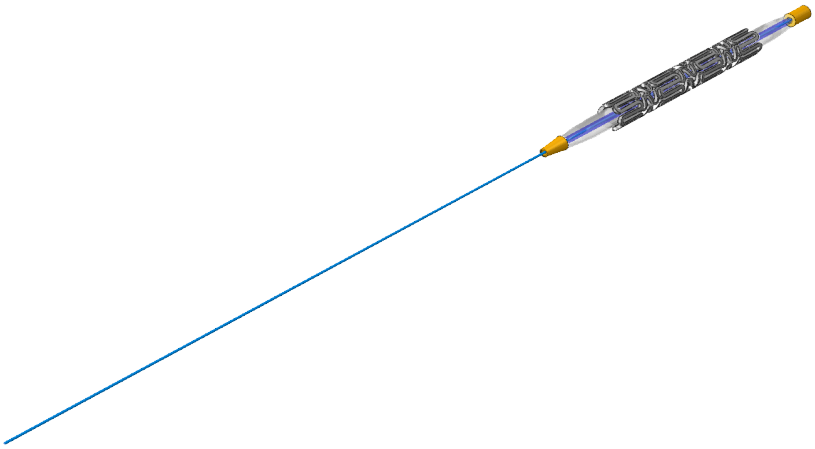

Figure 4.1: The stent/balloon model.

Also mesh definitions have remained the same, except, of course, the guide wire mesh. Guide wire has been divided 328 4-node 3-D bilinear rigid quadrilateral elements (R3D4).

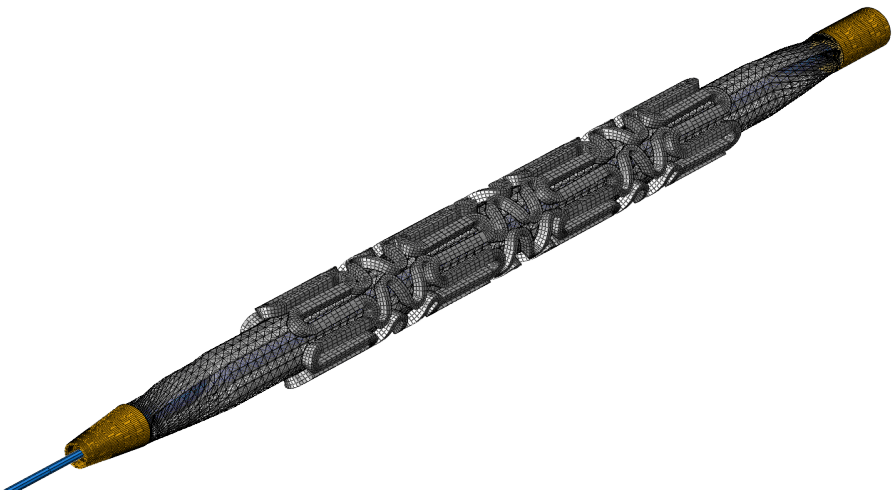

Figure 4.2: Mesh detail of the stent/balloon model.

Straight artery and plaque model

The straight segment of the atherosclerotic coronary artery was modeled as an idealized vessel and represented by a cylinder with outside diameter of 4mm and had a localized crescent-shaped axisymmetric stenosis with minimum lumen diameter of 2 mm, see Figure 4.3.

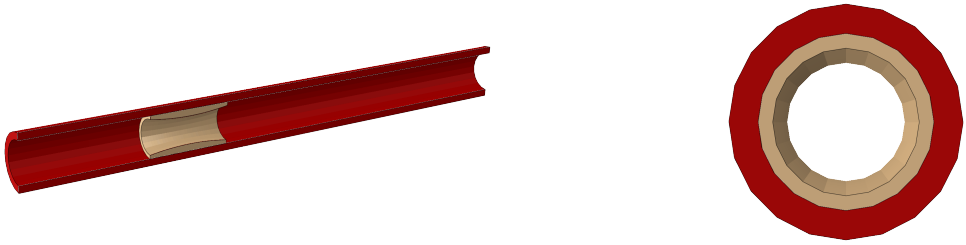

Figure 4.3: Atherosclerotic coronary vessel reconstruction.

The two materials of the artery wall, arterial tissue and stenotic plaque, were modeled using a 5-parameter third-order Mooney-Rivlin hyperelastic constitutive equation suggested by Lally et al. [22] and summarized in Table 4.1.

Coefficients	Arterial wall tissue (MPA)	Stenotic plaque tissue
C10	0.01890	-0.49596
C01	0.00275	0.50661
C11	0.8572	1.19353
C20	0.59043	3.63780
C30	0	4.73725

Table 4.1: Hyperelastic constants to describe the arterial tissue and stenotic plaque nonlinear elastic behavior[22]. These parameters describe a Mooney Rivlin model.

Increasing number of elements would lead to an elevate computational cost. Therefore the regions of the artery geometry subjected to minor deformations, i.e., the area from which the stent starts to move, during the stent expansion were meshed with larger elements, obtaining the mesh depicted in Figure 4.4.
The coronary artery and the stenotic plaque have been meshed with 8-node brick, reduced integration, elements (C3D8R). The coronary vessel mesh is composed by 6600 elements while the plaque mesh consists of 1800 elements. The thickness of the whole atherosclerotic artery has been portioned in three layers to better highlight the

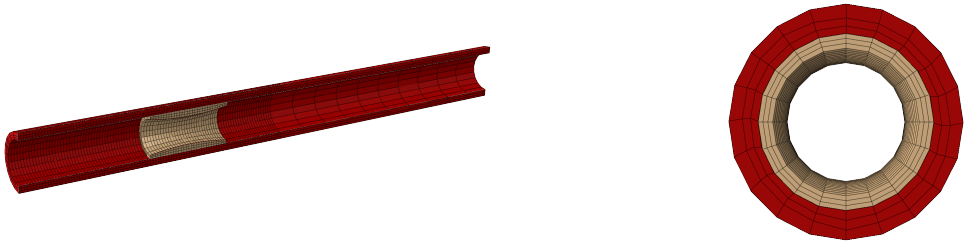

Figure 4.4: Atherosclerotic coronary vessel mesh.

nodal displacement as the stent deploys. Fixed displacement boundary conditions are imposed to both ends of the arterial vessel.

4.1.3 Numerical simulations

The whole simulation representing the stenting procedure is composed of four different steps:

- Crimping
- Insertion
- Deployment
- Balloon deflation

The ABAQUS/Explicit solver has been chosen again for the large deformation analysis, as this code provides a very stable general contact algorithm. Nevertheless the general contact algorithm, implemented in the Cypher stent expansion simulation to handle interactions between each components of the stent system (see Chapter 3), has been modified in order to allow the movement of the structure over the guide wire. A frictionless contact property has been then assigned to the pair composed by the inner surface of the catheter shaft and the surface of the guide wire, allowing the catheter shaft to easily scroll over the guide wire.

Different simulation time steps have been chosen. The stent has been, indeed, crimped in 0.001 seconds, since presented negligible dynamic effects while for the insertion step has been selected slower simulation time, 0.005 seconds. The analysis could not be faster since the inertial forces became dominant, indeed as the catheter shaft was moving, large deformations on the proximal tip occurred. The deployment and the balloon deflation steps have, instead, been chosen to last 0.01 seconds.

Crimping

The process in which the stent is crimped on the balloon is simulated by applying an increasing pressure on outer surface of the stent and, at the same time, on the inner surface of the balloon. The pressure applied on the stent starts from 0 N/mm^2 and reaches 1 N/mm^2 in order to reduce the stent diameter, whereas the pressure on the balloon varies in a very small range (0-0.0005 N/mm^2) to partially unfold the balloon without transferring the load to the stent. This step has been implemented in the simulation of the insertion of a stenting system, not only to simulate the real stent configuration, but also to enable a uniform movement of the entire structure. During the crimping step, both the balloon tips have been constrained to prevent the movement and the shortening of the balloon. The superelastic properties of the guide wire during the crimping and the insertion step has been neglected because the guide wire deformations are supposed to be small. For this reason the guide wire has been implemented as 3D rigid part instead of 3D deformable part and all the translational and rotational degrees of freedom of its reference point has been constrained.

Insertion

Insertion was simulated by enforcing a displacement at the proximal end of the catheter shaft to reach the stenotic plaque. To applied this displacement all the nodes of the proximal face of the cylindrical tip have been tied through multipoint constraint (MPC link). The multipoint constraint allows the motion of the slave nodes of a region to the motion of a single point. An additional equal displacement boundary condition and an equal multipoint constraint, have been imposed to the proximal stent end. Without this condition, it was impossible to adequately position the stent because sliding occurred between the balloon membrane and the inner stent surface. This sliding was due to insufficient frictional forces, although a pressure has been applied to the outer stent surface, prior to and during the insertion to mimic the stent fixation after crimping.

Deployment

In order to simulate the inflation of the inserted stent/balloon system, a model based on the results achieved in the insertion step has been developed. The multipoint constraint applied in the insertion step prevents the stent to deploy since each slave nodes is rigidly linked to the control point. Therefore the analysis could not be done with a unique simulation, since the multipoint constraint could not be inactivated before the last

step. For this reason all the parts, except the guide wire, has been imported from the insertion step in their deformed shape. The guide wire has, instead, been edited *ex novo* as a 3D deformable part and fixed at both ends since the guide wire, in the deployment step, undergoes higher deformations.
The simulation of the free expansion of the stent has been achieved by imposing an increasing uniform pressure starting from 0 N/mm^2 up to 2 N/mm^2 on the inner surface of the trifolded balloon. While importing the stent and the balloon from the insertion step, their state of stress has to be taken into account. Thanks to the Predefined Field Manager of the Load module of ABAQUS, all the stresses can be applied back to the parts imported.

Deflation

As previously stated, the balloon deflation has been included in the FE analysis to study the stent recoil due both to the stent material and to the pressure imposed by the elastic recoil of the vessel walls. In order to simulate the balloon deflation stage, has been applied a decreasing uniform pressure starting from 2 N/mm^2 down to 0 N/mm^2 on the inner surface of the trifolded balloon.

4.1.4 Results

The Figure 4.5 shows the two views of the stent delivery system before (left panel) and after crimping process (right panel). The stent crossing profile decreased from 1.15 mm to 1 mm as recommended by the manufacturer. The balloon, instead, took a 'dogboned' shape, i.e., the central region resulted thinner than the edges.
The insertion, deployment and deflation procedures for the Cypher stent in a straight coronary artery segment are visualized in Figure 4.7, Figure 4.8 and Figure 4.9, respectively.
As the stent delivery system has been correctly placed in the stenotic region, after the insertion the step, the balloon starts to inflate. Subsequently the stent deploys pressing the plaque against the artery walls, resulting in a deformed artery shape shown in Figure 4.6. It is outstanding how the stent adheres to the plaque pushing it back to restore patency to the stenosed vessel.
As the balloon is deflated, the radial strength of the stent is able to withstand the pressure imposed on it by the elastic recoil of the arterial walls.

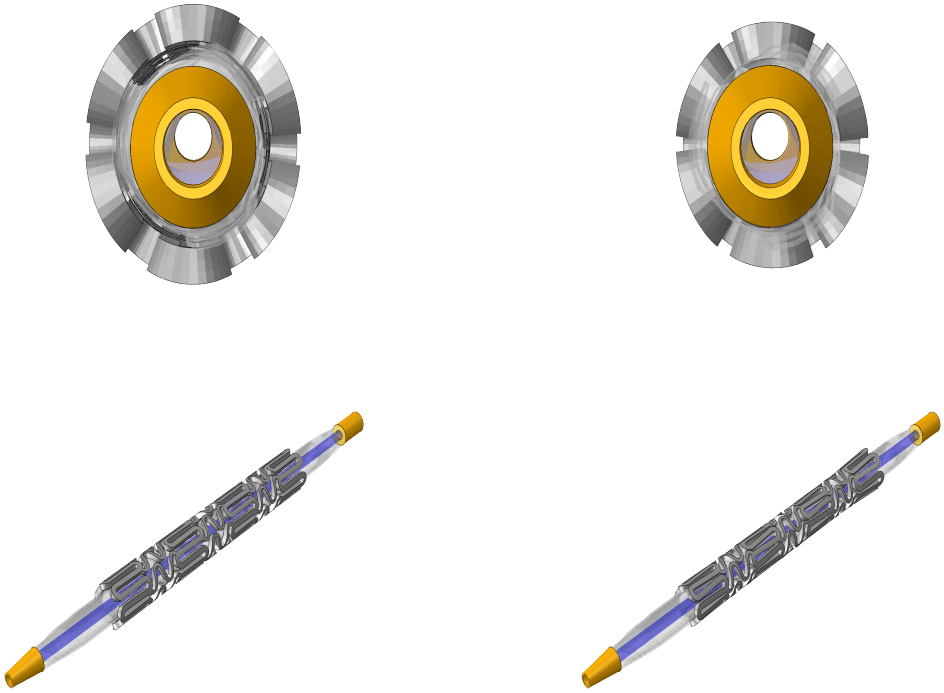

Figure 4.5: The Cypher stent crimping.

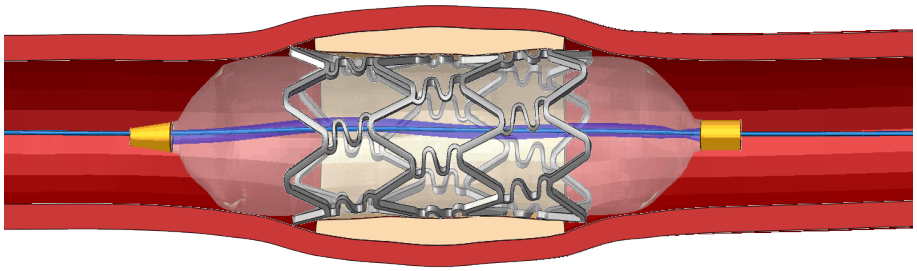

Figure 4.6: The atherosclerotic straight coronary artery deformed by the stents expansion.

(a) Time=0.0000 s.

(b) Time=0.0025 s.

(c) Time=0.003750 s.

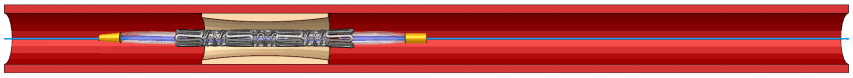

(d) Time=0.01 s.

Figure 4.7: The Cypher stent insertion in a straight coronary artery segment. From the top to the bottom different steps of the stent deflation are illustrated.

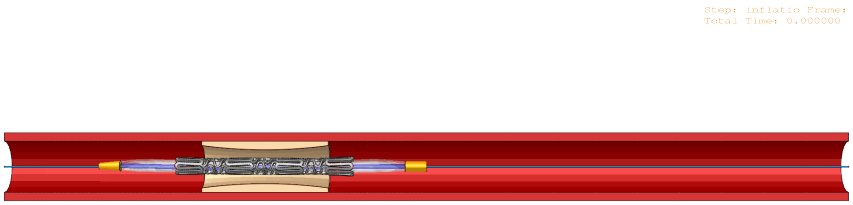

(a) Time=0.0000 s.

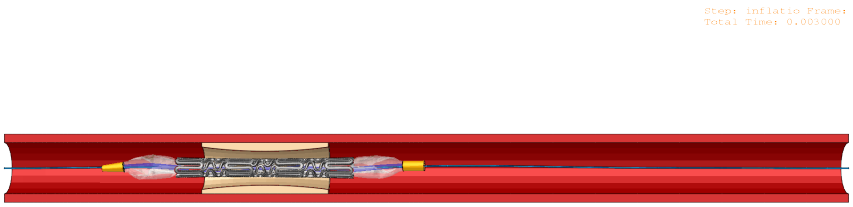

(b) Time=0.003 s.

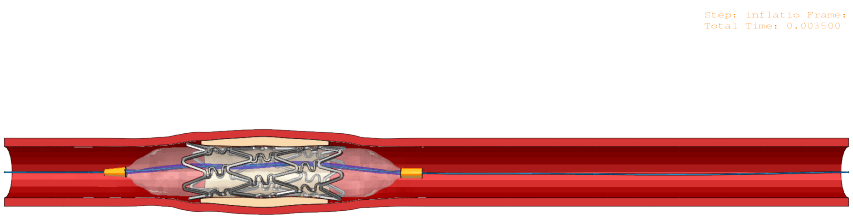

(c) Time=0.0035 s.

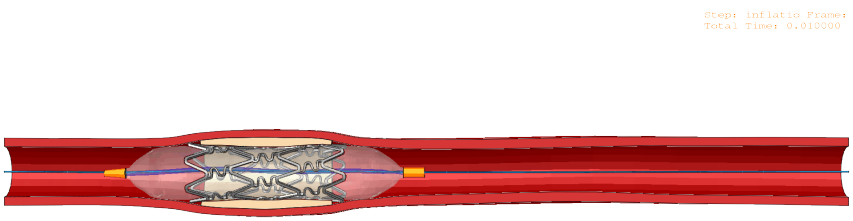

(d) Time=0.01 s.

Figure 4.8: The Cypher stent inflation. From the top to the bottom different steps of the stent deflation are illustrated.

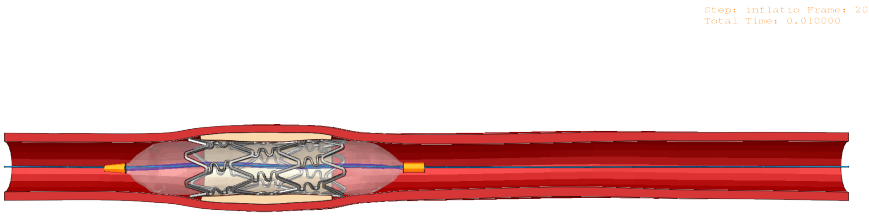

(a) Time=0.01 s.

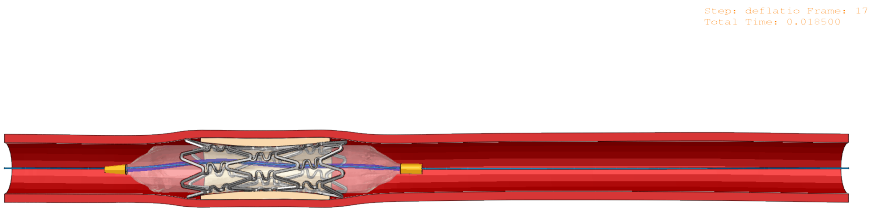

(b) Time=0.0185 s.

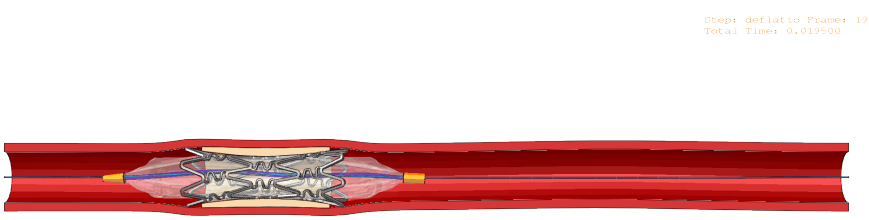

(c) Time=0.0195 s.

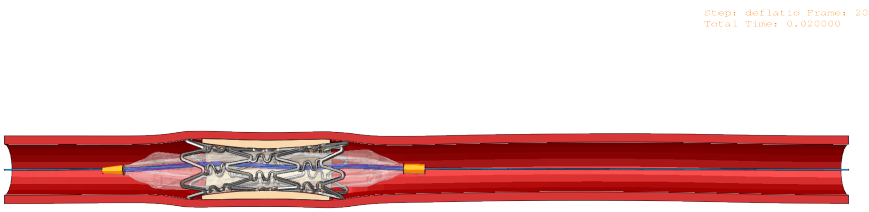

(d) Time=0.02 s.

Figure 4.9: The Cypher stent deflation. From the top to the bottom different steps of the stent deflation are illustrated.

4.2 Stent insertion and deployment in a curved coronary artery segment

Coronary arteries, as stated in Chapter 1, are small tortuous vessels, therefore the stent has often to be deployed into curved coronary segments.
The insertion of a stent system in a straight coronary vessel has been developed in order to be the ground on which build the simulation of the insertion of the stent delivery system in a curved coronary artery. Therefore the same procedures, implemented to create the simulation of the insertion in a coronary straight vessel, have been applied, exception, obviously, with the atherosclerotic coronary artery model, which is below presented and with the guide wire since it has to be placed into curved vessel.

4.2.1 Curved Artery and Plaque model

As done for the straight coronary artery segment, the CAD model of the atherosclerotic curved vessel has been idealized and drawn with Rhinoceros. The Figure 4.10 shows the artery and the plaque sketches.

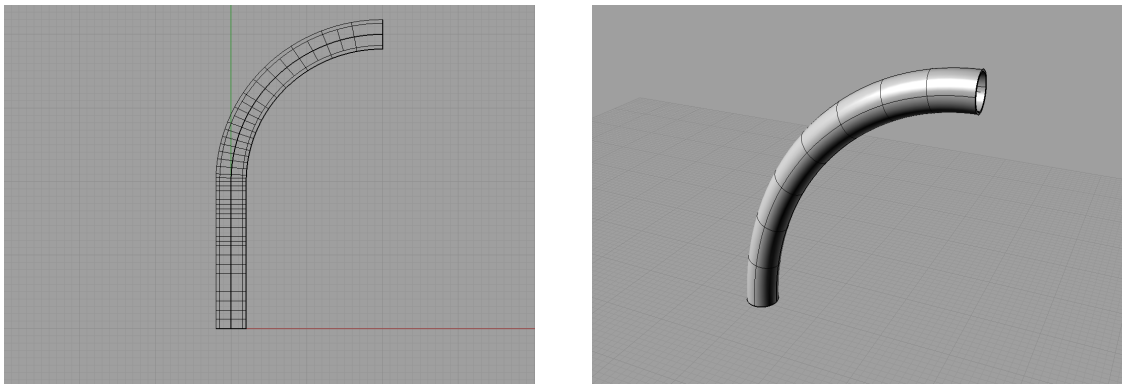

Figure 4.10: Atherosclerotic coronary curved vessel reconstruction carried out with Rhinoceros.

The curved artery segment has been sketched as a cylindrical pipe whose straight segment, 20 mm long, turns following a quarter-circle arc with a radius of 20 mm. The inner and the outer diameters of the vessel measures the same of the diameters of the straight segment (see section 4.1.2).
In order to simplify the designing phase, the plaque has been considered to lay in the entire curve of the artery, instead of laying in the middle section. Therefore the plaque

has been drawn 20 mm long and 20 mm high with a crescent inner diameter reaching its maximum of 2 mm.
The curved coronary artery segment and the plaque have been discretized using 8-node brick, reduced integration, elements (C3D8R), 2400 elements for the vessel and 800 for the plaque. Same material definitions applied in section 4.1.2 have been implemented for the curve atherosclerotic coronary artery. In Figure 4.11 the meshes of the stenotic vessel can be visualized.

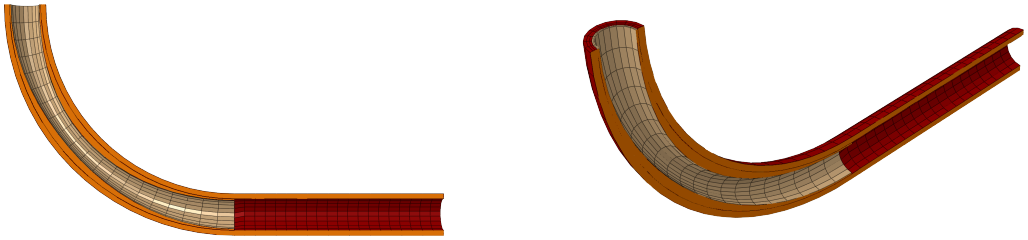

Figure 4.11: Atherosclerotic coronary curved vessel mesh performed in ABAQUS.

4.2.2 Simulation results

The stent insertion and deployment in a curved coronary artery segment model, as in a straight coronary artery segment model, are characterized by four different stages: (i) the stent crimping, (ii) the stent delivery system insertion, (iii) the stent deployment and (iv) the balloon deflation. The whole model of the stent delivery system placed in a curved coronary artery segment is depicted in Figure 4.12.
The insertion, deployment and deflation procedures for the Cypher stent in a curved coronary artery segment are visualized in Figure 4.14, Figure 4.15 and Figure 4.16, respectively. As the stent delivery system has been correctly placed in the stenotic curved region (last picture of the Figure 4.14), the balloon starts to inflate. Subsequently the stent deploys pressing the plaque against the artery walls, resulting in a deformed artery shape shown in Figure 4.13.
Implantation of the coronary stent changes the three-dimensional vessel geometry significantly. In particular, a straightening effect of the stented vessel can be observed in Figure 4.15 (bottom picture). The arterial wall is subject to high dynamic effects as shown in the deflation step (Figure 4.16). Furthermore, unlike the results achieved with the stent deployment in a straight vessel, the balloon deflation causes the radial retraction of the stent under the pressure applied by the arterial walls.

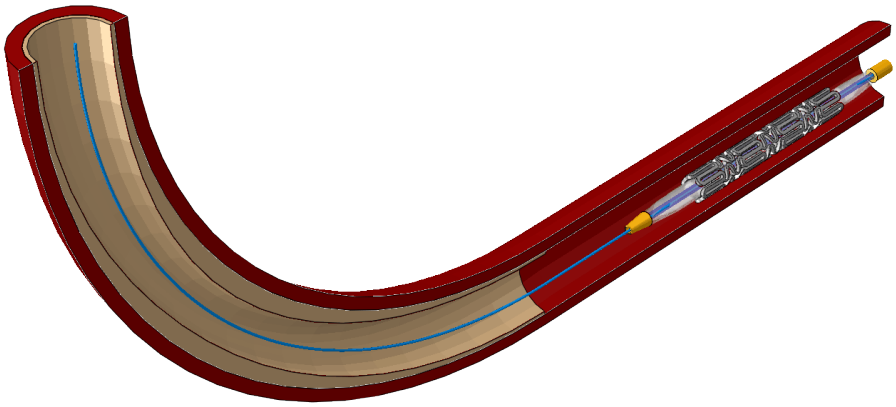

Figure 4.12: The stent delivery system placed in a curved coronary arerty segment.

4.3 Limitations and Discussion

The main limitation encountered with this modeling techniques is that the atherosclerotic arteries in which the stents are implanted are an idealized representation of stenosed coronary arteries. Despite the results achieved in the straight coronary artery, i.e., minimal elastic recoil, a realistic model of the atherosclerotic artery is required.
The availability of generating patient-specific stenotic geometries overcomes this problem. The feasibility of generating patient-specific stenotic models based on high-resolution images of *ex-vivo* tissue samples might overcome this problem.
An additional limitation of our model is the absence of any rupture mechanism in the arterial components.
A simulation strategy considering the insertion of a stent system over a guide wire in a straight and in a curved coronary artery has been proposed. In Table 4.1 are summarized the main positive results and drawbacks encountered by modeling the insertion and the deployment of a stent delivery system in an atherosclerotic coronary artery segment, both straight or curved.

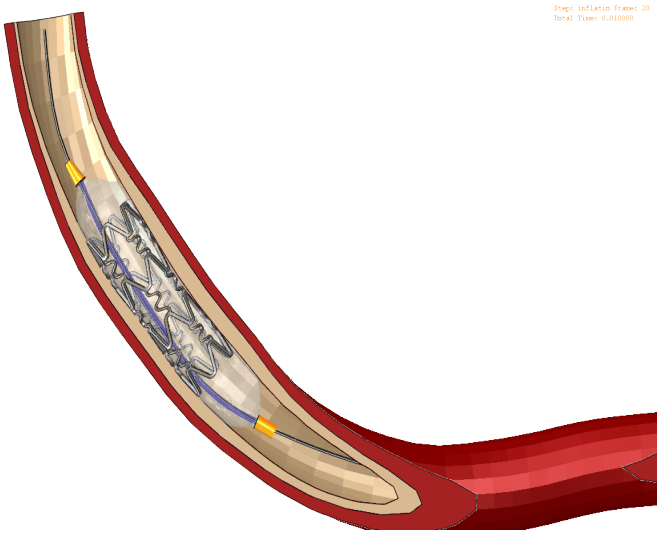

Figure 4.13: The atherosclerotic curved coronary artery deformed by the stens expansion.

Stenoses artery typology	Posivite aspects	Drawbacks
Straight coronary vessel	Great adhesion No significative elastic recoil	Idealized plaque geometry
Curved coronary vessel	Accurately positioned Straightening effects	Idealized plaque geometry Dynamic effects

Table 4.2: Positive aspects and drawbacks of the proposed model of the insertion and deployment of a stent delivery system in coronary arteries.

The limitations presented in Table 4.2 can be overcome quite easily. Concerning the dynamic effects, increasing the simulation time would certainly reduce the unwanted floating movement of due to the inertial forces (see Figure 4.15). With regards to the plaque model, the availability of angiographic images would allow a more accurately reconstruction of the atherosclerotic vessel and thus more accurately analysis.

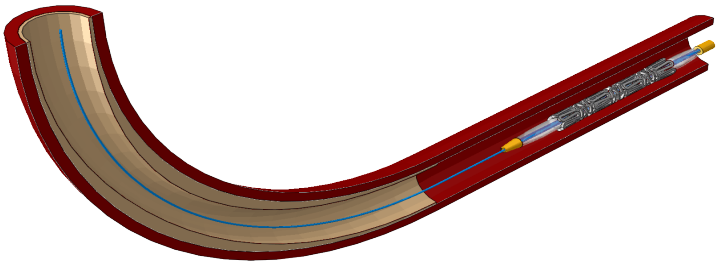

(a) Time=0.001 s.

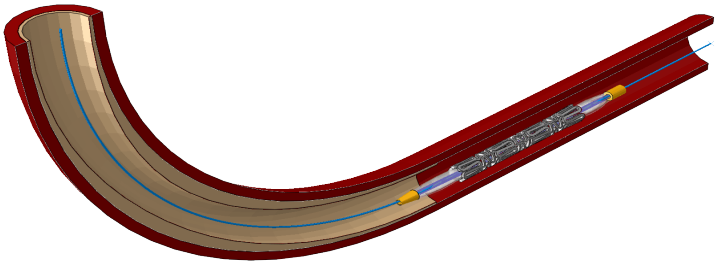

(b) Time=0.0045 s.

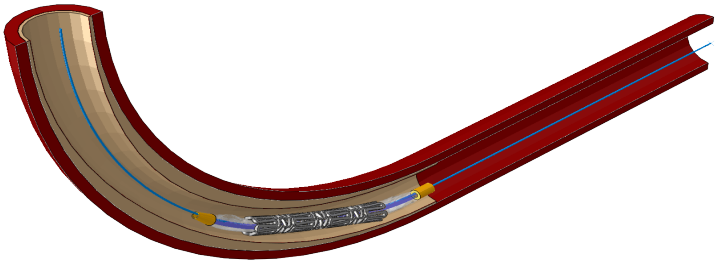

(c) Time=0.007 s.

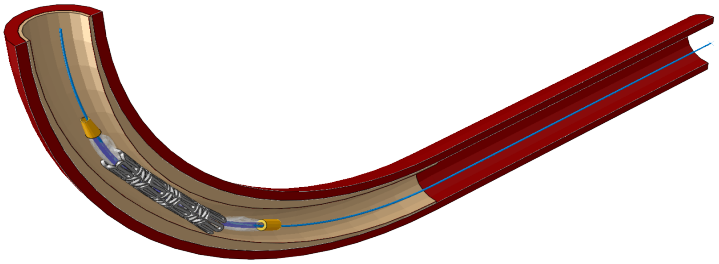

(d) Time=0.01 s.

Figure 4.14: The Cypher stent insertion in a curved coronary artery segment. From the top to the bottom different steps of the stent deflation are illustrated.

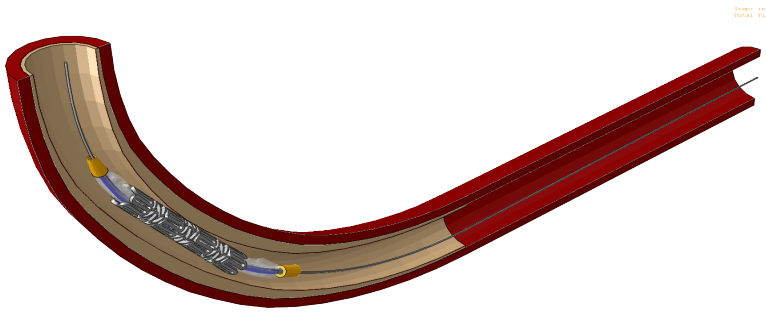

(a) Time=0.0015 s.

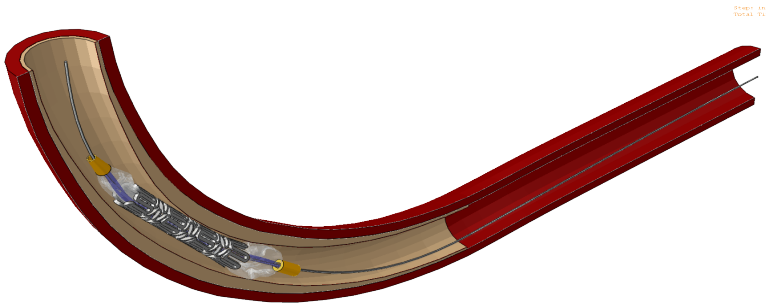

(b) Time=0.0035 s.

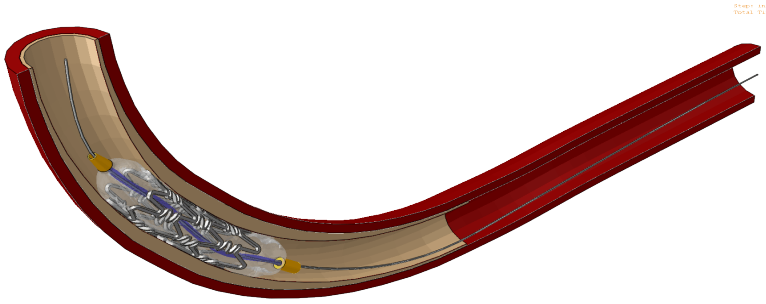

(c) Time=0.004 s.

(d) Time=0.007 s.

Figure 4.15: The Cypher stent inflation. From the top to the bottom different steps of the stent deflation are illustrated.

(a) Time=0.014 s.

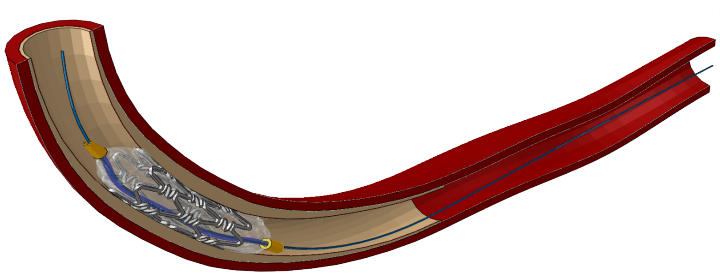

(b) Time=0.019 s.

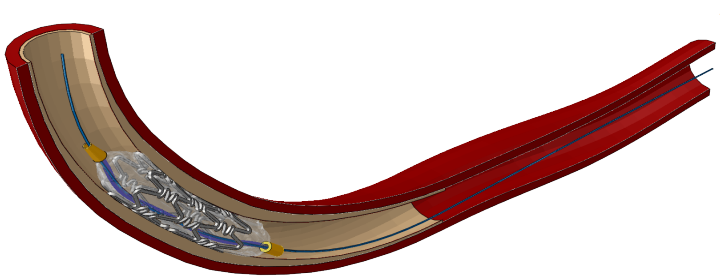

(c) Time=0.0195 s.

(d) Time=0.020 s.

Figure 4.16: Cypher stent deflation. From the top to the bottom different steps of the stent deflation are illustrated.

4.4 The Element stent: expansion modeling

In this section a three-dimensional stent model of the *Element* coronary stent[1] has been created. The commercially available Element coronary stent is crimped on a five-folded balloon. Two different simulation of the stent expansion have been carried out: one with a trifolded balloon obtained from micro-CT scans and one with an idealized five-folded balloon.

4.4.1 Material and methods

The five-folded balloon

Micro-CT images of the real balloon of the Element stent system were not available. Data provided by the manufacturer were the balloon length, the compliance chart and the folding pattern. It has been then developed an idealized five-folding pattern using the graphical finite element preprocessor ABAQUS/CAE. The idealized five-folded balloon presented a folded diameter of 0.65 mm in balloon straight body, which decreases to 0.4 mm on the balloon circular end. The length of the non-tapered cylindrical part is 26 mm, while the complete balloon measures 28 mm from proximal to distal balloon tip and the uniform balloon thickness is considered to be 0.037 mm.

(a) Balloon folded section sketch.

(b) Balloon semi-section sketch.

Figure 4.17: The Element idealized five-folded balloon model reconstructed in ABAQUS.

The trifolded balloon

Beside the creation of the five-folded balloon, a realistic trifolded balloon based on micro-CT scans has been implemented. The balloon has been reconstructed from the

[1] from Boston Scientific Corp., USA

available Micro-CT images of the Tryton balloon (Tryton medical,Inc., Durham, North Carolina). The procedure to obtain the balloon geometry from micro-CT images has been explained in Chapter 2. The balloon obtained has the same length of the five-folded balloon but the tapered ends are longer (1.5 mm) and the ends diameter is a little larger (0.5 mm), in order to avoid the interactions due the decreasing diameter. The balloon has been resized to have the same crossing profile of the idealized five-folded balloon.

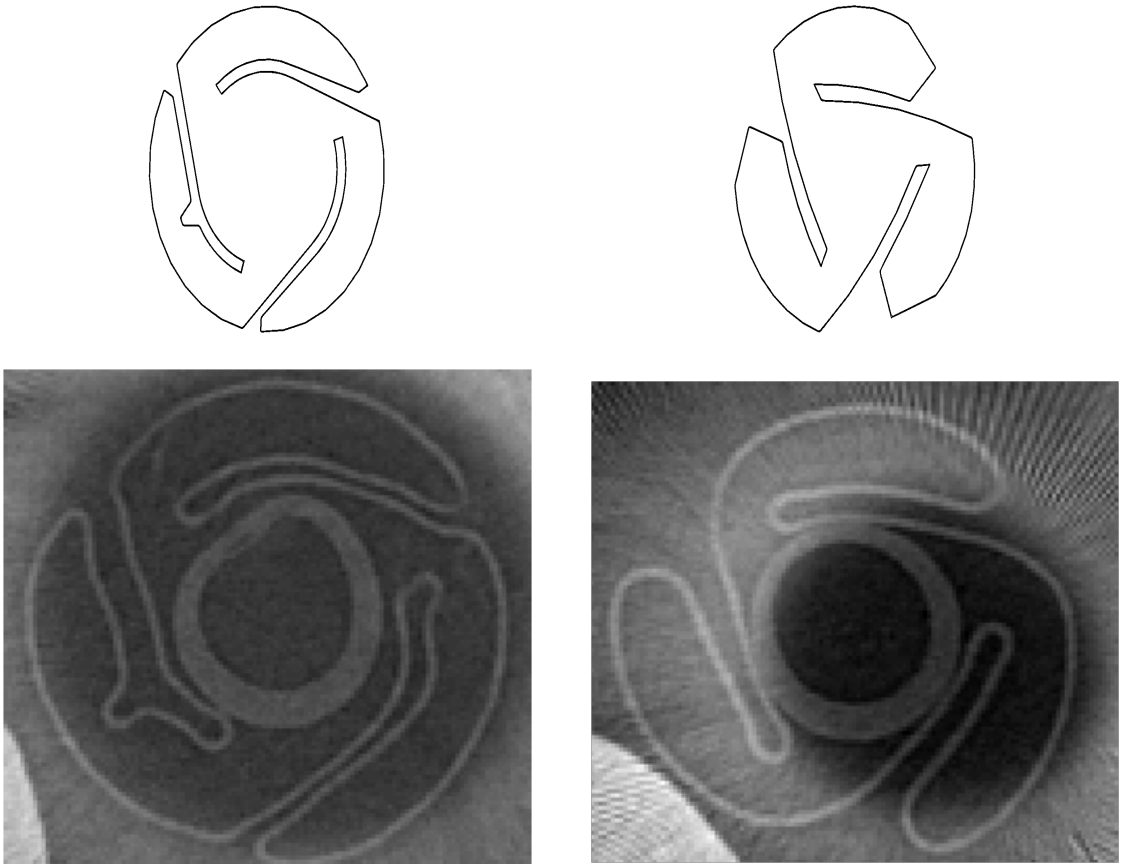

Figure 4.18: Comparison between the ABAQUS sketches and micro-CT images of two different section of the Tryton balloon.

The balloon material is a 72 durometer Pebax for the Promus Element. The material is bi-directionally orientated during the balloon forming process. The Young's modulus has been derived from the compliance chart, as done previously for the Sprinter balloon. The material is characterized by a Young's modulus of 326 N/mm^2, a Poisson's ratio of 0.4 and a density of 1350 g/cm^3.
The five-folded balloon mesh consists of 55600 (M3D3) 3-node triangular membrane

elements, while the trifolded balloon has only 29440 elements.

(a) Entire balloon. (b) Cross-sectional view of the balloon.

Figure 4.19: The Element idealized five-folded balloon model reconstructed in ABAQUS.

(a) Entire balloon. (b) Cross-sectional view of the balloon.

Figure 4.20: The Element realistic trifolded balloon model reconstructed in ABAQUS.

The Stent

The Element geometry has been reconstructed from a STL file produced with Osirix as described in Chapter 2. This coronary stent has a nominal length of 24 mm and a nominal diameter of 3 mm. The inner and outer diameter of the crimped stent are 0.893 mm and 1.055 mm respectively, resulting in 0.162 mm (0.006") of thickness as provided by the manufacturer.
The stent has been meshed with three-dimensional 8-node brick 'reduced-integration' elements (C3D8R) using ABAQUS finite element code. A finite element mesh consisting of 127425 elements was used for the Element stent.
The balloon expandable Element stent is manufactured in a special proprietary material, the PtCr. Only the yield stress of the PtCr was available, 480 N/mm^2. Knowing the yield stress is possible to calculate the elastic modulus since the yield stress corresponds to the stress applied to obtain a deformation of 0.002. The Young's modulus

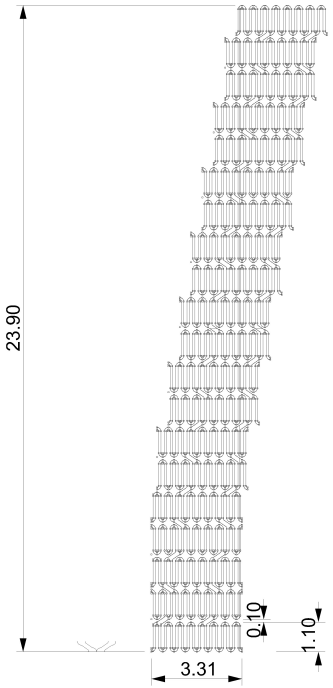

(a) Planar sketch of the Element stent from Rhinoceros.

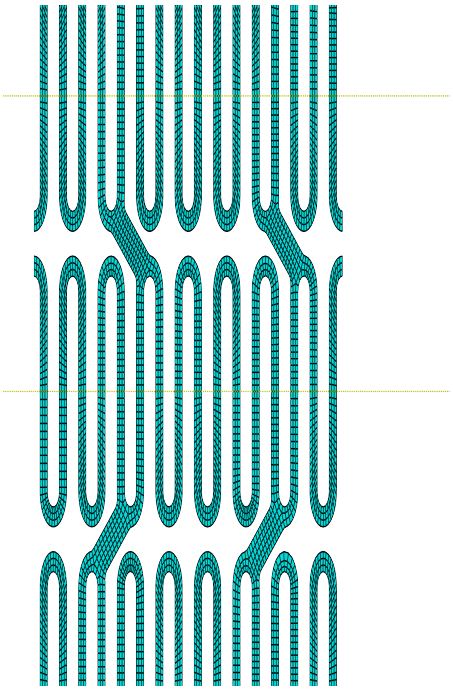

(b) Detail of the planar mesh of the Element stent from ABAQUS.

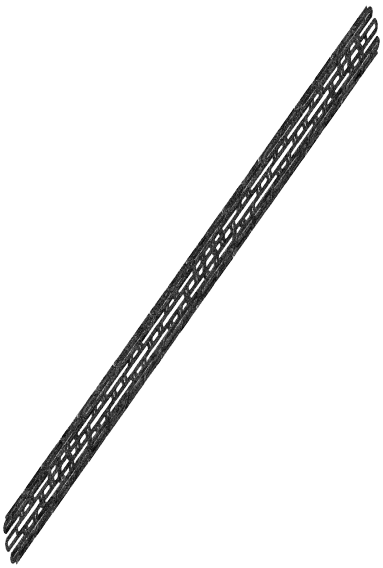

(c) Entire meshed stent.

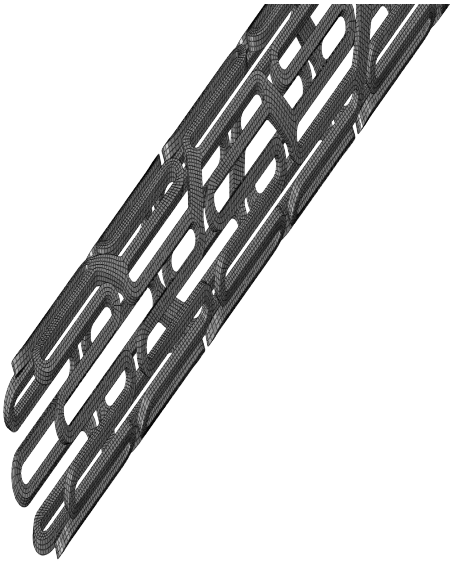

(d) Zoom of the stent mesh.

Figure 4.21: Reconstruction of the Element stent.

achieved, the Poisson's ratio and the density are then supposed to be 240000 N/mm^2, 0.3 and 9900 g/cm^3, respectively.

Tips and the catheter

The two short tubular tips are assumed to measure 1 mm in length while the inner diameter is chosen to be 0.22 mm, the same as the diameter of the catheter tube, since they are connected. The cylindrical tip outer diameter measures as the balloon end diameter, i.e., 0.4 mm for the model with the five-folded balloon and 0.5 mm for the one with the trifolded balloon. The conical tip outer diameter, instead, decreases from the balloon end diameter to 0.3 mm.
The catheter tube and the tips are characterized by a linear elastic material with a Young's modulus of 1000 MPa, a Poisson's ratio of 0.4 and density of 940 kg/m^3, as previously stated.
The catheter tube was modeled with 6400 four-node doubly curved thin or thick shell, reduced integration elements (S4R). Both the cylindrical and the conical tips have been meshed with 1600 C3D8R elements, the same as the stent.

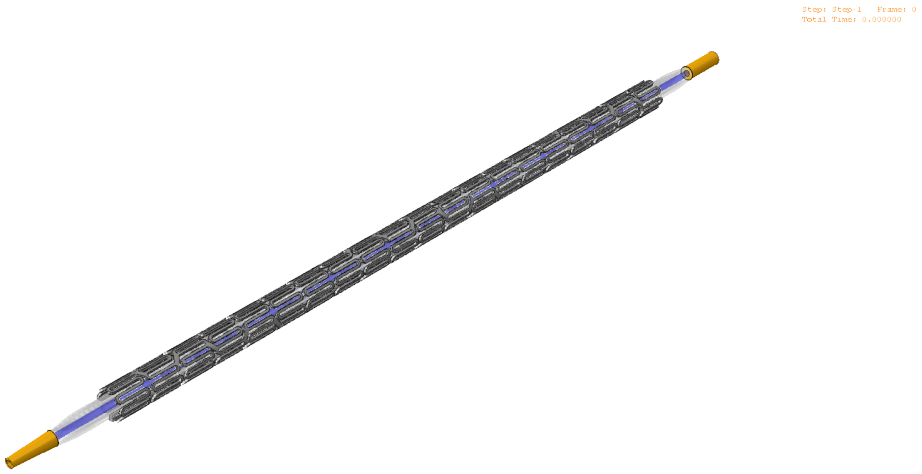

Figure 4.22: The whole Element stent delivery system model.

Boundary conditions and loads

An increasing uniform pressure starting from 0 N/ mm^2 up to 1.5 N/ mm^2 has been applied on the inner surface of both the balloons.

Both ends of the balloons have been tied with tips extremities in order to prevent the balloon movement but allowing its expansion. Boundary condition has been then applied to both the tips. All the translational degrees of freedom have been constrained on the proximal face of the cylindrical tip and on the distal face of the conical tip thus preventing the movement and the shortening of the balloon. Catheter and tips have been also tied together to create the catheter shaft.

4.4.2 Results

The simulations results are shown in Figure 4.23; on the left panel is visualized the expansion of the Element stent crimped on a realistic trifolded balloon, while on the right panel is depicted the Element stent crimped on a idealized five-folded balloon. As can be easily seen, the simulation including the trifolded balloon shows better results in terms of final shape than the simulation with the five-folded balloon. Indeed the Element stent correctly deploys when is expanded by a realistic trifolded balloon whereas the stent seems to twist when is expanded by an idealized five-folded balloon while having the same step time (0.01 s). These results suggest, one more time, that realistic balloons should be implemented even if presenting different folding pattern. Despite the close agreement with the expanded shape, the Element stent deployed by the trifolded balloon does not follow the compliance chart since it presents a smaller diameter as the diameter provided by the manufacturer while the compliance chart from the five-folded balloon, despite the uncorrect final shape, is closed to the data provided by the manufacturer.

4.4.3 Conclusions

Different simulations, involving different balloon geometries, have been carried out to study the Element stent expansion. The first simulation is based on creation of an idealized five-folded balloon as suggested by manufacturer. Despite the final shape of the stent seems to be correct, the whole system deploys partially. Subsequently a simulation, based on the 3D reconstruction of a realistic model trifolded balloon, has been developed showing better agreement with the compliance chart provided by manufacturer but appears dominated by dynamic effects. The differences between these simulations suggest that the proper balloon should be applied to the proper stent, i.e., balloons used to deploy stents should be reconstructed by the micro-CT images of the

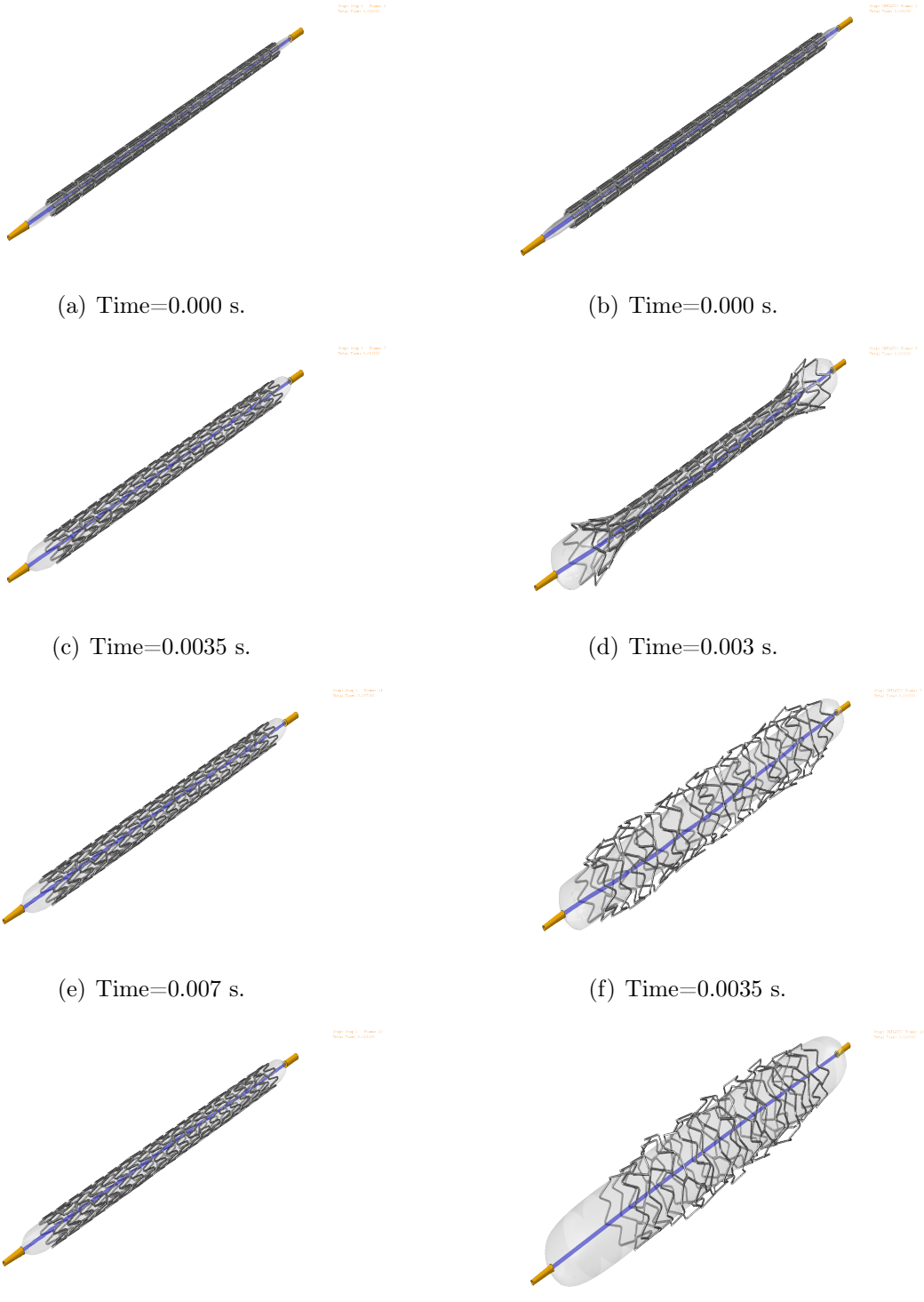

(a) Time=0.000 s.

(b) Time=0.000 s.

(c) Time=0.0035 s.

(d) Time=0.003 s.

(e) Time=0.007 s.

(f) Time=0.0035 s.

(g) Time=0.01 s.

(h) Time=0.01 s.

Figure 4.23: The Element deployment; left panel: the Element expansion driven by the inflation of a realistic trifolded balloon model, right panel: the Element expansion driven by the inflation of idealized five-folded balloon model.

specific stent.

4.5 The Tryton stent: expansion modeling

There is a tendency for atherosclerosis to develop at specific arterial sites such as bifurcations and curvatures and this has been related to the specific blood flow patterns at those locations [24]. In order to model stents deployment into bifurcations, the Tryton bifurcational stent model has implemented. Both the stent and balloon micro-CT images has been available so a realistic model of the Tryton deployment has been developed.

4.5.1 Material and methods

The Tryton stent model, reconstructed through the process described in section 2.4, is shown in Figure 4.24, whereas the trifolded balloon has just been reconstructed in the previous section (section 4.4) and is depicted in Figure 4.20.
The particular shape of the Tryton, especially the great opening-the side branch access-between the stent struts, that can be easily seen, is designed to leave the space in which another balloon would pass to widen the stenosed bifurcation.

The balloon

The 3D reconstructed trifolded balloon presented a folded diameter of 1.066 mm, which decreases to 0.62 mm on the balloon circular end. The complete balloon measures 22 mm from proximal to distal balloon tip while the length of the non-tapered cylindrical part is 19 mm and the uniform balloon thickness is considered to be 0.02 mm. The balloon has been meshed with 23040 (M3D3) 3-node triangular membrane elements and is assumed to be fabricated by Duralyn, the same material of the Raptor balloon, an hypothesis to simplify the simulation.

The stent

The Tryton geometry has been reconstructed from a STL file produced with Osirix as described in Chapter 2. This bifurcational stent has a nominal length of 19 mm. The Tryton stent presents a crossing profile of 1.4 mm and an inner diameter of 1.1 mm,

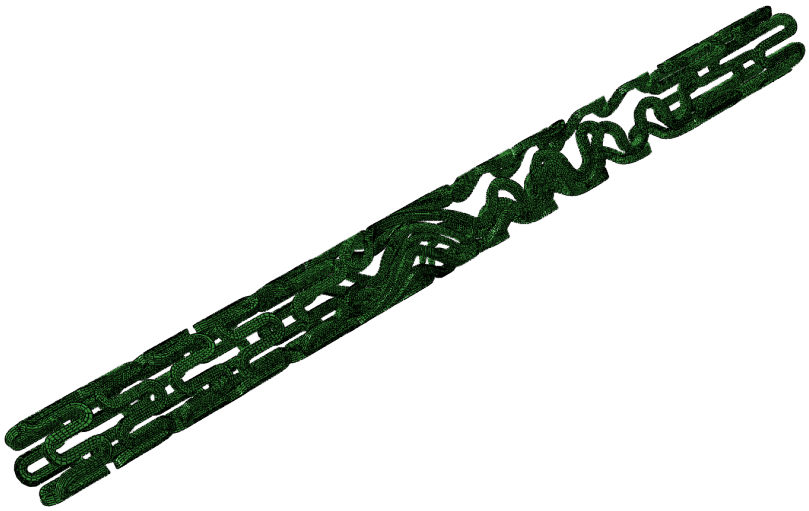

Figure 4.24: The Tryton stent model.

resulting in 0.3 mm of thickness. The stent has been meshed with three-dimensional 8-node brick 'reduced-integration' elements (C3D8R) using ABAQUS finite element code. A finite element mesh consisting of 64772 elements has been applied to the Tryton stent.
The bifurcational Tryton stent is manufactured by Cobaltum- Cromium material (CoCr). The Young's modulus, the Poisson's ratio and the density have been imposed to be 233000 N/mm^2, 0.35 and 8700 g/cm^3, respectively.

Tips and catheter

The two short tubular tips are assumed to measure 1.5 mm in length while the inner diameter is chosen to be 0.3 mm, the same as the diameter of the catheter tube, since they are connected. The cylindrical tip outer diameter measures as the balloon end diameter, i.e., 0.62 mm. The conical tip outer diameter, instead, decreases from the balloon end diameter to 0.44 mm.
As already stated the catheter tube and the tips are supposed to be fabricated in polyethylene and therefore characterized by a Young's modulus of 1000 MPa, a Poisson's ratio of 0.4 and density of 940 kg/m^3.

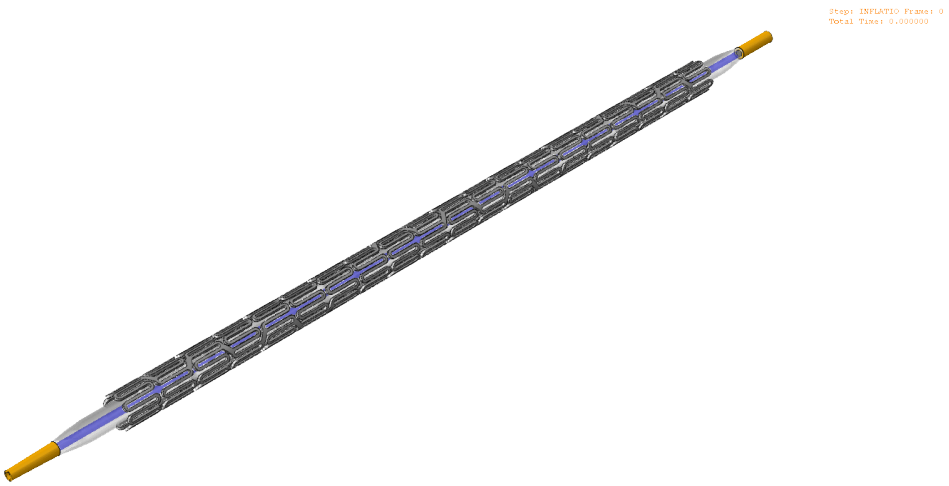

Figure 4.25: The whole Tryton bifurcational stent delivery system model.

4.5.2 Results

Two simulations, with different step time, have been carried out and are shown in Figure 4.26 and in Figure 4.27. The Tryton bifurcational stent has been deployed by applying an increasing uniform pressure starting from 0 N/ mm^2 up to 1.5 N/ mm^2 on the inner surface of the balloon.
The stent expands in a proper manner thus allowing an hypothetical widening of a atherosclerotic bifurcation lesion.
The stent deploys first in the region where the stent struts leave more space within each other; this site lets the balloon unconstrained so the initially balloon expansion begins in this very space, as can be visualized in Figure4.26. No significant difference can be seen between the simulation implemented with a time step of 0.001 s and the one with a time step of 0.01 s.

4.5.3 Conclusions

The correct expansion of the Tryton bifurcational stent seems to be promising in future simulations of the insertion and deployment of this stent into bifurcation stenosis. The lack of differences between the simulations implemented with different time steps confirms that the proper 3D reconstructed balloon model placed inside the proper 3D reconstructed stent model, is the right way to follow.

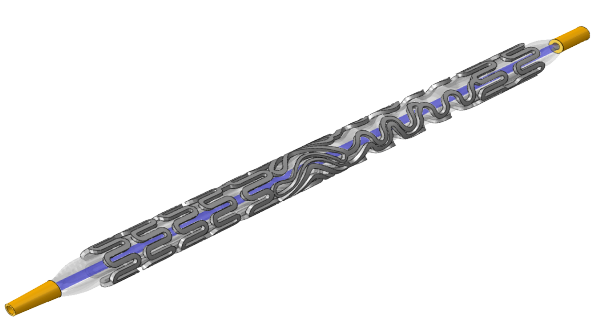

(a) Time=0.000 s.

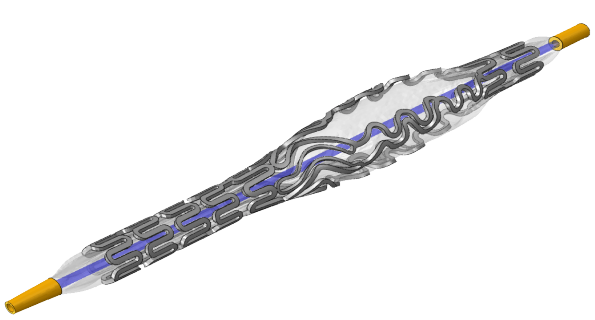

(b) Time=0.0015 s.

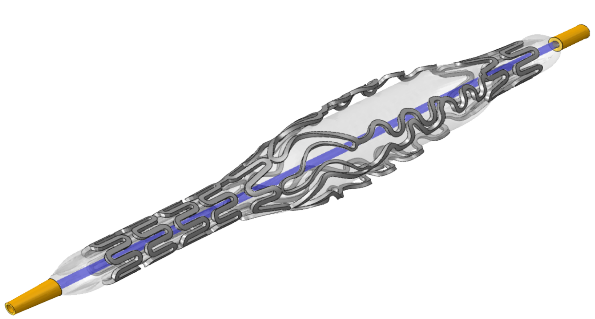

(c) Time=0.0035 s.

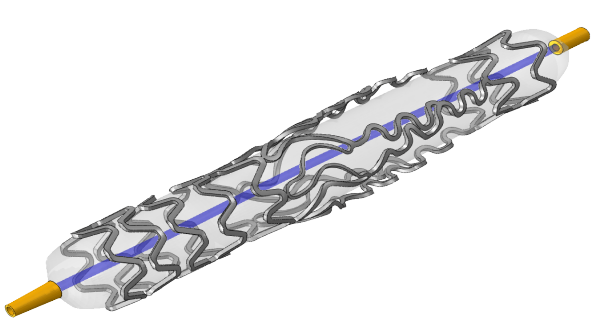

(d) Time=0.01 s.

Figure 4.26: The Tryton stent inflation simulation with time step= 0.001. From the top to the bottom can be seen different steps of the stent inflation.

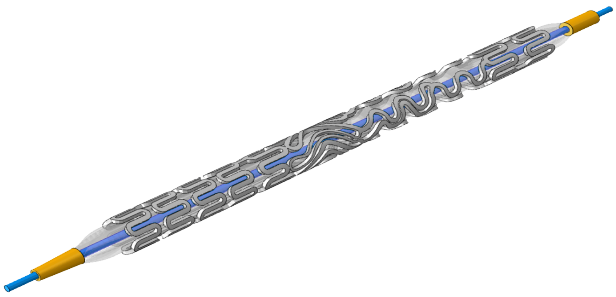

(a) Time=0.000 s.

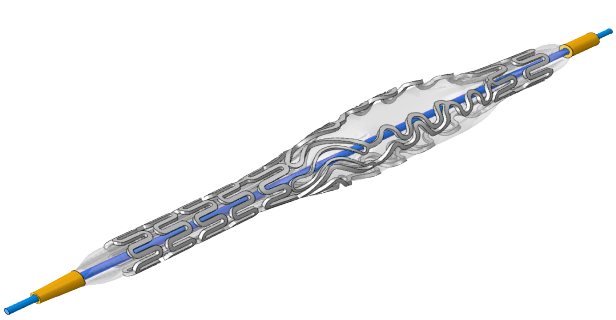

(b) Time=0.0015 s.

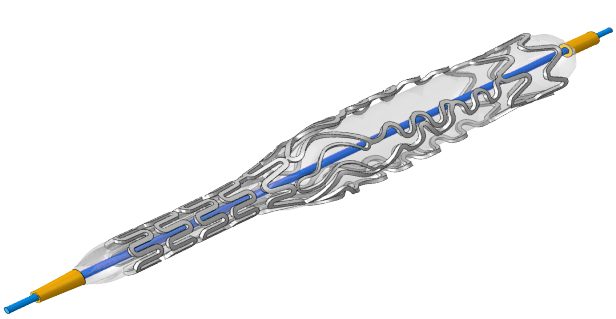

(c) Time=0.0035 s.

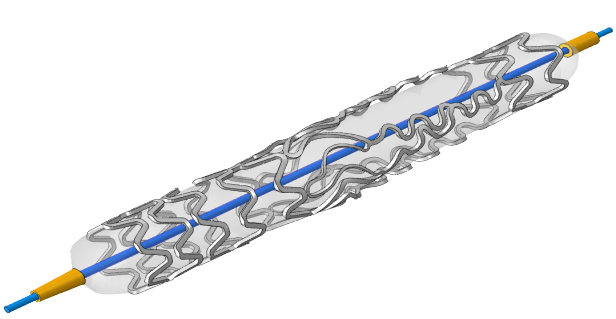

(d) Time=0.01 s.

Figure 4.27: The Tryton stent inflation simulation with time step= 0.01. From the top to the bottom can be seen different steps of the stent inflation.

4.6 Conclusions

A simulation strategy considering the insertion of a stent system over a guide wire in a straight and in a curved coronary bifurcation has been proposed.
Implantation of the stents changes the three-dimensional vessel geometry significantly. The deployment of the Cypher stent, after having it positioned into a straight segment of the atherosclerotic coronary artery, has proved to be very promising since the plaque is pressed against the arterial walls restoring the patency of the stenosed vessel.
The curved segment of the three-dimensional coronary artery model has been less widen, instead, but it has been straightened after implantation of the stent. Including the artery in the simulation models can also be useful to investigate the impact of the presence of the artery on the obtained stent diameters, since it has been observed using intravascular ultrasound that in clinical practice, the stents will only reach on average 75% of the predicted diameter, as a consequence of complex interactions with the atherosclerotic plaque forming the coronary stenosis [24]. The main limitation encountered in this model is that the arteries in which the stents are deployed are an idealized representation of stenosed coronary arteries.
Simulations with patient-specific geometries obtained by medical imaging or less idealized plaque geometry would certainly improve the implemented model.
Further works will include modeling of patient-specific stenosed vessel in order to simulate the implantation of different stent typologies in curved coronary arteries and bifurcations, allowing the results comparison to better choose which the most correct stent should be implanted.

Chapter 5

Conclusions and further developments

Within this thesis, it has been created a virtual design space to investigate the mechanics of stent implantation within atherosclerotic coronary arteries using the finite element method. This design tool is applicable to balloon expandable stents in a variety of materials (stainless steel, cobalt-chromium, PtCr, etc.) and designs. The work described in this thesis provides also an interesting strategy to investigate the complex problem of insertion and deployment of stents within stenosed vessels. Some suggestions for future research are also included as this work is certainly not an endpoint.

5.1 Conclusion

In **Chapter 2** the key characteristics of the stent delivery system have been presented in order to have a wide overview of how this structure is made of and how it works. Especially attention has been paid to the dimensions, designs and materials properties of both the balloon and the stent. Achieved this basic knowledge, it is possible to create a model to investigate the mechanical behavior of the stents. Several stent expansion numerical simulations have been carried out, mainly based on the Finite Element Method. The FEA offers, indeed, numerous possibilities in the simulation of coronary stenting procedure since modeling tools should be able to accurately predict the most important stent characteristics (e.g. expansion, recoil, dogboning, foreshortening, flexibility, stiffness, etc.). In order to generate a realistic stent delivery system model, a methodology based on the stent/balloon reconstruction from micro-CT scans has been developed. Implementing realistic stent models is the starting point for the evaluation and comparison of different models of the free expansion of balloon expandable stents.

The finite element model that allows to investigate the free expansion of balloon-expandable stents is described in the **Chapter 3**. First an angioplasty folded balloon model, based solely on the manufacturer's compliance chart data, has been developed and simulated. The proposed methodology takes into account the balloon tapering as they plays a important role in the unfolding process. The numerical results of the free expansion of folded angioplasty balloons, in terms of pressure and diameter, show very good agreement with data provided by the manufacturer and consequently the proposed balloon model is an essential prerequisite to study realistic balloon/stent interactions. Subsequently the complete stent system model has been implemented. In this model have been included the catheter, the guide wire and the tips in order to get closer to the reality. This model could act as a solid basis to study and optimize the mechanical behavior of balloon-expandable stents as the numerical results correspond very well with both qualitative and quantitative manufacturer data. The efficiency and accuracy of the developed procedure is illustrated for the Cordis's Cypher stent.

A simulation strategy considering the insertion of a folded balloon catheter over a guide wire has been developed in **Chapter 4**, in order to position the stents within straight and curved atherosclerotic coronary arteries. It has become clearly during the reading of this work, that the stenting procedure's target is to widen occluded arteries. Despite simulations of the free balloon expandable stent expansion provides interesting data, such as the expansion pattern, the elastic recoil of stent struts, the dogboning effect, etc., the merely stent deployment without the presence of the stenosed vessel can result useless to physicians as they are asked to choose the most suitable stent for the patient-specific lesion. Developing models of the stent insertion and deployment into stenosed vessels is the basis to implement an incredible tool able to select which is the most appropriate stent to implant. This tool would use a stent library, composed by different -varying in designs and materials- stents, each one available in all the commercialized sizes, and patient-specific angiography images to catch the accurate geometry of the atherosclerotic artery. The main limitation of the model proposed in Chapter 4 is that the arteries in which the stents are deployed are an idealized representation of stenosed coronary arteries.

5.2 Future prospects

The findings and methods of this thesis can be used as a starting point for further research topics. Without the aim of being complete, some suggestions are made in this section.
In the immediate future several developments could be implemented; from the wide variety of possibilities that the virtual design space provides, the very first steps that could be done are pointed out as follows:

- Reconstruction of different stent models from micro-CT images: (Xience Prime and Integrity) thus starting to populate the stent library, as said in Chapter 2;
- Reconstruction of dedicated balloons with 3/6 folding pattern in order to make available different balloon models;
- Development of the entire delivery system for each reconstructed stent;
- Stent system deployment in curved coronary artery;
- Stent system deployment into idealized bifurcation;
- Stent system deployment into patient-specific bifurcation;
- Comparison of different stents in the same anatomy.

The growing number of available stents, indeed, increases the freedom for the physicians to choose from, but it also brings along the question of which stent to use for which particular case/type of stenosis: different design, different impact. For example, a very flexible stent with a low crossing profile may be required to treat patients with highly tortuous vessels. Therefore, objective comparisons of these devices are needed in terms of pharmacological effect, thrombogenicity, geometrical aspects of the design, and mechanical performance among many others, because all of these parameters are important for optimal stent selection. Simulations with patient-specific geometries, that accurately reproduce the in vivo curvatures of the vessel segment, obtained by medical imaging or less idealized plaque geometry would certainly improve the implemented model. Therefore further works will include modeling of patient-specific stenosed vessel in order to simulate the implantation of different stent typologies in curved coronary arteries and bifurcations, allowing the results comparison to better choose which the most correct stent should be implanted.

Besides the early advancements, just suggested, an infinite list of proposals can be made to further improve the models developed in the stenting modeling field. Therefore, it has been listed a few items:

- Introduction of the drug kinetic. Nowadays most of stents are drug-eluting stents. The drug kinetic should be included in the numerical studies to get closer to reality.
- Automation of simulations. The process of the stent reconstruction, although seems to be simply feasible , is currently time-consuming. Therefore, automation of this process is a very important step to increase the value of these simulations.
- Better integration of computer simulation with experimental data. Most of the numerical studies on the stenting procedure are characterized by the lack of experimental evidence, creating a missing-link with reality and provoking skepticism.
- The remodelling of the vessel wall after stent implantation is a time-dependent process. Including this temporal component in the simulations would be very interesting.

The suggestions, made in this final remark, would themselves be the starting point for further developments in this recent field, whose domain has no boundaries.

List of Figures

List of Tables

Bibliography

[1] J. Mackay and G. Mensah. The Atlas of Heart Disease and Stroke. Deaths from coronary heart disease. Accessed March 11, 2011. `http://www.who.int/cardiovascular_diseases/en/cvd_atlas_14_deathHD.pdf`, 2004.

[2] S. J. George and J. Johnson. *Atherosclerosis: Molecular and Cellular Mechanisms*. Wiley-VCK, 2010.

[3] O. Hügli M.Togni S. Cook, A. Walker and B. Meier. Percutaneous coronary interventions in europe. prevalence, numerical estimates, and projections based on data up to 2004. *Clinical Research in Cardiology*, 96:375–382, 2007.

[4] D. S. Baim and W. Grossman. *Grossman's Cardiac Catheterization, Angiography, and Intervention, 6th ed*, page 7. AHA, 2000.

[5] M. R. Reynolds, N. Neil, K. K. L. Ho, R. Berezin, R. S. Cosgrove, R. A. Lager, C. Sirois, R. G. Johnson, and D. J. Cohen. Clinical and economic outcomes of multivessel coronary stenting compared with bypass surgery: A single-center US experience. *American Heart Journal*, 2003.

[6] P. W. Serruys, M. C. Morice, A. P. Kappetein, A. Colombo, D. R. Holmes, M. J. Mack, E. Ståhle, T. E. Feldman, M. Van den Brand, E. J. Bass, N. Van Dyck, K. Leadley, and Dawkins, Keith D. and F. W. Mohr. Percutaneous coronary intervention versus coronary-artery bypass grafting for severe coronary artery disease. *New England Journal of Medicine*, 360:961–972, 2009.

[7] J. Booth, T. Clayton, J. Pepper, F. Nugara, M. Flather and U. Sigwart. Randomized, Controlled Trial of Coronary Artery Bypass Surgery Versus Percutaneous Coronary Intervention in Patients With Multivessel Coronary Artery Disease: Six-Year Follow-Up From the Stent or Surgery Trial (SoS). *Circulation*, 118:381–388, 2008.

[8] G. Pertici. Stent state of art. *Innovare*, 4:38–43, 2006.

[9] J. E. Calvin J. E. Parrillo F. Q. Almeda, N. Sandeep and L. W. Klein. Frequency of abrupt vessel closure and side branch occlusion after percutaneous coronary intervention in a 6.5-year period (1994 to 2000) at a single medical center. *The American Journal of Cardiology*, 89(10):1151 – 1155, 2002.

[10] D. J. Fischman. A randomized comparison of coronary-stent placement and balloon angioplasty in the treatment of coronary artery disease. *The new England Journal of Medicine*, 331:496–501, 1994.

[11] P. W. Serruys, and P. De Jaegere. A comparison of balloon-expandable-stent implantation with balloon angioplasty in patiens with coronary artery disease. *The new England Journal of Medicine*, 331:489–495, 1994.

[12] B. O'Brien and W. Carroll. The evolution of cardiovascular stent materials and surfaces in response to clinical drivers: A review. *Acta Biomaterialia*, 5(4):945 – 958, 2009.

[13] T. Htay and W. Ming Liu. Drug-eluting stents: a review and update. *Vascular Health and Risk Management*, 1:263–276, 2005.

[14] M. Schier P. Erne and T. Resink. The road to bioabsorbable stents: Reaching clinical reality? *CardioVascular and Interventional Radiology*, 29:11–16, 2006.

[15] J. Tobis V. Spanos, G. Stankovic and A. Colombo. The challenge of in-stent restenosis: insights from intravascular ultrasound. *European Heart Journal*, 24:138–150, 2003.

[16] M. De Beule. *Finite Element Stent Design.* PhD Thesis, Ghent University, Belgium, 2008.

[17] M. Otsuka F. Kolodgie S. Yazdani, M. Nakano. and R. Virmani. Atheroma and coronary bifurcations: before and after stenting. *EuroIntervention Supplement*, 6:J24–J30, 2010.

[18] C. Thomson A.M. Matthew, M. Kieran and L. Zollikofer. *Image-Guided Intervention*, pages 42–43. Saunders Elsevier, 2008.

[19] M. A. Saab. Application of high-pressure balloons in the medical device industry. Accessed March 30, 2011. http://www.advpoly.com/Documents/MedicalBalloonPaper.pdf, 1999.

[20] I. A. López L. E. Mulero L. A. Alicea, J. I. Aviles and 2011. L. A. Sánchez. Accessed April 3. Mechanics biomaterials: Stents. http://academic.uprm.edu/~mgoyal/materialsmay2004/f04stents.pdf, 2004.

[21] C. Bonsignore D. Stoeckel and 2011. S. Duda. Accessed April 9. A survey of stent designs. http://www.nitinol.com/media/reference-library/009.pdf, 2002.

[22] F. Dolan C. Lally and P.J. Prendergas. Cardiovascular stent design and vessel stresses:a finite element analysis. *Journal of Biomechanics*, 38:1574–1581, 2005.

[23] S. Schievano L. Socci L. Petrini A. Thury J. J. Wentzel A.F. van der Steen P. W. Serruys F. J. Gijsen, F. Migliavacca and G. Dubini. Simulation of a stent deployment in a realistic human coronary artery. *BioMedical Engineering OnLine*, 7:1574–1581, 2008.

[24] P. Mortier. *Computer Modeling of Coronary Bifurcation Stenting*. PhD Thesis, Ghent University, Belgium, 2010.

[25] MathWorks Website: http://www.mathworks.com/products/matlab/description1.html.

[26] Medtronic Website:http://www.medtronic.com/for-healthcare-professionals/products-therapies/cardiovascular/catheters/balloon-dilatation-catheters/nc-sprinter-rx-noncompliant-balloon-dilatatio index.htm#tab2.

[27] Stent Research Unit of Ghent University Website:http://www.stent-ibitech.ugent.be/downloads/downloads.htm.

[28] M. De Beule D. Van Loo Y. Taeymans P. Segers P. Verdonck P. Mortier, G.A. Holzapfel and B. Verhegghe. A Novel Simulation Strategy for Stent Insertion and Deployment in Curved Coronary Bifurcations: Comparison of Three Drug-Eluting Stents. *Annals of Biomedical Engineering*, 38:88–99, 2010.